

Nuclear magnetic resonance of rare-earth Van Vleck paramagnets

L. K. Aminov and M. A. Teplov

V. I. Ul'yanov Lenin State University, Kazan'

Usp. Fiz. Nauk **142**, 49–82 (September 1985)

Theoretical and experimental investigations of nuclear magnetic resonance in rare-earth Van Vleck paramagnetic materials are reviewed. The majority of the observed aspects of the phenomenon is explained by the interaction of nuclei with the residual electronic magnetic moment in the singlet ground state and the modulation of this interaction as a result of the coupling of the electronic moments among themselves and with the oscillations of the crystal lattice, and also by various spin-spin interactions involving enhanced nuclear moments. At liquid helium and higher temperatures the most significant effect is the modulation of the hyperfine interaction resulting from real thermal transitions of Van Vleck ions between the ground state and the nearest excited states. Within the framework of a single simple theory based on the randomly varying in time hyperfine interaction Hamiltonian, a description is given of the temperature dependence of the shifts and widths of NMR lines, of the spin-lattice relaxation times of nuclei within Van Vleck ions and within diamagnetic atoms, and also of the frequency and orientation dependences of these quantities. The theory is in agreement with experiment not only qualitatively, but to a significant extent also quantitatively without resorting to any adjustable parameters. Some special features of nuclear magnetism of Van Vleck paramagnetic materials at ultralow temperatures are also considered.

CONTENTS

Introduction.....	762
1. Fundamental properties of Van Vleck paramagnets and their use in ultra-low-temperature technology.....	763
a) Electronic and nuclear paramagnetism. b) Distinctive features of nuclear magnetic resonance. c) Nuclear magnetic cooling.	
2. Spin-spin interactions.....	769
a) Interaction of 4f electrons with nuclei of diamagnetic ligands. b) Interaction of nuclei of Van Vleck ions with one another. c) Interaction of nuclei of Van Vleck ions with diamagnetic ligand nuclei and with paramagnetic ions. d) Nuclear resonance line broadening of Van Vleck ions. e) Transport of thermally excited 4f electron states.	
3. Nuclear magnetic relaxation.....	773
a) Resonance lineshapes under adiabatic conditions. b) Relaxation of nuclei of rare-earth ions caused by rapid fluctuations of the hyperfine fields. c) Relaxation of nuclei of diamagnetic atoms. d) Relaxation via paramagnetic impurities. e) One-phonon relaxation processes and nuclear acoustic resonance.	
Conclusion.....	781
References.....	781

INTRODUCTION

Van Vleck paramagnetism is as ubiquitous as diamagnetism; however, it exhibits far more diversity in its manifestations than does the latter. This is because the Zeeman effect usually appears as a small perturbation of a system's energy spectrum, the gross features of which are determined by interactions far stronger than the magnetic ones. Whereas diamagnetism affects the system energy through a term quadratic in the applied magnetic field, Van Vleck paramagnetism affects it through linear terms which are treated by second-order perturbation theory. The great variety of zero-order spectra a system can have (and hence the intermediate states available) thus predisposes the Van Vleck paramagnetism to take on a huge range of possible values. By custom, one refers to a material as a Van Vleck paramagnet if

it has no magnetic moment in the ground electronic state but has a paramagnetic susceptibility far in excess of its diamagnetic susceptibility. Striking examples of Van Vleck paramagnets are afforded by crystals which contain rare-earth ions with an even number of electrons in their unfilled 4f shells, i.e., Pr^{3+} , Eu^{3+} , Tb^{3+} , Ho^{3+} , and Tm^{3+} . The ground-state multiplet $^{2S+1}L_J$ of these ions is often split by the crystal field so that the lowest levels are singlets or non-magnetic doublets, while the excited levels are separated from the ground state levels by intervals of the order of $10\text{--}100\text{ cm}^{-1}$. The isotopes ^{141}Pr , ^{159}Tb , ^{165}Ho , and ^{169}Tm are present in 100% abundance, and have non-zero nuclear spin; therefore, compounds of these elements exhibit not only electronic but also nuclear magnetism. Paramagnetic ("chemical") shifts of the nuclear magnetic resonance (NMR) lines in such systems, as a rule, are strongly aniso-

tropic and attain immense values right up into the hundreds. This leads to interesting peculiarities in the magnetic resonance of the nuclei of rare earth ions, which permit one to classify their resonance behavior as intermediate between the usual NMR and EPR.

The first researcher to turn his attention to the above-mentioned peculiarities was S. A. Al'tshuler; following his suggestions, Zaripov¹ carried out calculations of the NMR characteristics of Van Vleck systems. Independently, Elliott² also carried out calculations on the spectra of ¹⁵¹Eu and ¹⁵³Eu in europium ethyl sulfate. Experimentally, resonance was first observed in corundum, where it was due to impurity ions of ⁵¹V³⁺.³ NMR of RE ions in the singlet state was first detected in 1967.⁴ Al'tshuler also pointed out that it was possible to use Van Vleck paramagnets to obtain ultralow temperatures.⁵ The implementation of this proposal by Andres and Bucher in intermetallic rare earth compounds^{6,7} generated additional interest among physicists in this class of materials. And, while the earliest systematic investigations of the NMR of Van Vleck paramagnets were carried out within the confines of the University of Kazan,^{1,3-5,8-15} at the present time these phenomena are being studied at a whole series of scientific centers specializing in the areas of magnetism and low temperature physics (see e.g., Refs. 16-21).

The characteristic energy level pattern for RE ions with Stark splitting of the ground multiplet in the crystal field—i.e., an ensemble of narrowly-spaced levels with energy intervals of the order of 10-100 cm⁻¹—leads also to a series of other peculiarities of rare-earth compounds, in particular structural instabilities in the low-temperature regime. These instabilities manifest themselves in the form of the cooperative Jahn-Teller effect (see the review of Ref. 22), the giant magnetostriction observed in a series of crystals,^{23,24} anomalies in elastic constants,^{25,27} and finally the distinctive field and temperature dependences of EPR linewidths for impurity ions.^{28,29} Naturally, the NMR spectra and relaxation characteristics of rare-earth Van Vleck paramagnets bear the imprint of all the wealth of physics of the materials under investigation; thus, a correct interpretation of the results of a NMR study of these materials is of general interest to physicists.

Recent works in this field have established a common viewpoint from which one can interpret the general pattern of nuclear magnetic resonance and relaxation in dielectric systems with singlet ground states. The key elements of this pattern prove to be the fluctuating hyperfine interactions between nuclei and electrons in the unfilled 4f shells of the RE ions. The present review is also devoted to an exposition of ideas and insights which have recently been accumulating in this area of physics; Semën Alexandrovich Al'tshuler, a corresponding Member of the Academy of Sciences of the USSR, is the initiator and guiding spirit behind all the investigations and results presented herein. In the first section of the review, the questions under discussion pertain for the most part to the origins of the intrinsic NMR spectra of nuclei of RE ions with singlet ground states (in the future, for brevity we will call these ions "Van Vleck ions"). A discus-

sion of the fundamental physical ideas is presented here along with illustrations of the very striking peculiarities which characterize the phenomena in question. The second section is devoted to an analysis of the various interactions which give rise to broadening of the resonance lines. The third section contains an examination of that part of the NMR line width and spin-lattice relaxation that are due to rapid fluctuations of the hyperfine interactions, which in turn are for the most part a consequence of the migration of electronic excitations of the system. Other relaxation mechanisms are also discussed here.

Insofar as our goal is to elucidate the distinctive features of the NMR spectra and relaxation characteristics of Van Vleck ions, we have consciously restricted ourselves to a selection of specific topics of study, choosing to investigate two crystals in which these distinctive features are most strikingly evident—thulium ethyl sulfate, Tm(O₂H₅SO₄)₃ × 9H₂O (TmES), and thulium lithium difluoride LiTmF₄. In view of the aforementioned goals we have set, this is for a number of reasons an optimum choice of crystals. First of all, the crystals TmES and LiTmF₄ are dielectrics; this fact frees us from the necessity of including effects due to electrical conductivity. Secondly, these crystals possess rather high symmetry (trigonal and tetragonal, respectively) and their structures have been studied in detail. Thirdly, the crystal-line electric field acting on the Tm ion also possesses rather high symmetry, and the energy levels and wave functions of the Tm³⁺ ion are well-known. Fourthly, the ¹⁶⁹Tm nucleus has no electric quadrupole moment; this allows us to avoid unnecessary complications connected with the effects of quadrupole interactions. The above-mentioned circumstances allow us to determine with maximum precision the degree of reliability of our theoretical models; the detailed computational procedure used for the specific compounds we have chosen is in turn applicable to arbitrary dielectrics. As regards intermetallic Van Vleck paramagnets, the qualitative features of their behavior are similar to those of dielectrics although here the RE ions are essentially coupled by superexchange through the conduction electrons, and this keeps us from making precise quantitative estimates. We refer those readers who are interested in details of the NMR spectra of Van Vleck ions in dielectric crystals to the original articles: Pr₂(SO₄)₃·8H₂O,^{4,11,30-32} Pr(NO₃)₃·6H₂O,³⁰ Pr(ReO₄)₃·4H₂O,³⁰ PrF₃,^{20,33} PrAlO₃,³⁴ PrVO₄,^{35,36} Cs₂NaPrCl₆,³⁷ Cs₂NaTbCl₆,³⁷ HoVO₄,³⁸ Rb₂NaHoF₆,³⁹ Tm₃Ga₅O₁₂,⁴⁰ Tm₃Al₅O₁₂,⁴¹ TmVO₄,⁴²⁻⁴⁴ TmPO₄,⁴⁴⁻⁴⁶ Cs₂NaTmCl₆,³⁷ TmAsO₄.⁴⁷ The relatively rare case of a system whose ground state is a nonmagnetic doublet is encountered in the cubic crystal Cs₂NaHoCl₆.⁴⁸ Information about NMR in intermetallic rare-earth compounds can be found in Refs. 49-55, 21.

1. FUNDAMENTAL PROPERTIES OF VAN VLECK PARAMAGNETS AND THEIR USE IN ULTRALOW-TEMPERATURE TECHNOLOGY

a) Electronic and nuclear paramagnetisms

Our first concern will be to calculate the magnetization of RE Van Vleck paramagnets. Let us write down the Hamil-

tonian for the Van Vleck ion in question separately, in the form

$$\begin{aligned} \mathcal{H} &= \mathcal{H}_0 + \mathcal{H}', \mathcal{H}' = \mathcal{H}_{eZ} + \mathcal{H}_{IZ} + \mathcal{H}_{IJ} \\ &= g_J \mu_B \mathbf{HJ} - \gamma_I \hbar \mathbf{HI} + A_J \mathbf{JI}. \end{aligned} \quad (1.1)$$

The Hamiltonian \mathcal{H}_0 determines the ion's electronic energy level structure in the absence of a magnetic field. Provided that we confine ourselves to investigating the rare-earth ions alone, we need only deal with that group of levels which arises from the crystal-field splitting of the ground-state multiplet $^{2S+1}L_J$ of the free ion. The remaining multiplets, as a rule, are separated from the ground-state multiplet by an energy interval of the order of 10^4 – 10^5 cm^{-1} , while the total splitting of the separate multiplets is of the order of 10^3 cm^{-1} . Under these circumstances we are justified in writing down the electronic Zeeman energy \mathcal{H}_{eZ} and hyperfine interaction \mathcal{H}_{IJ} in the form (1.1). The term \mathcal{H}_{IZ} of the perturbation \mathcal{H}' in (1.1) is the nuclear Zeeman energy, μ_B is the Bohr magneton, g_J is the Landé g -factor and γ_I is the nuclear gyromagnetic ratio. If the nuclear spin is $I > 1/2$, then the perturbation must also include the nuclear quadrupole energy \mathcal{H}_{IQ} ; it does not change the general pattern of the phenomenon in any essential way, but introduces quantitative complications into the calculation; therefore in what follows we will not write it out explicitly.

The energy spectrum determined by \mathcal{H}_0 , and the corresponding wave functions (in the JM_J representation) can be calculated with the help of this or other models of the crystal fields, or found from experiment. TmES (thulium ethyl sulfate) will serve as a typical example of a crystal in which the lowest electronic state of the RE ion is a singlet; the energy levels of the Tm^{3+} ion (3H_6) and wave functions are displayed in Table I. One can find analogous tables for LiTmF_4 in Refs. 26, 57. A model electron-nuclear spectrum is shown in Figure 1. In the absence of the perturbation \mathcal{H}' , this spectrum consists of a ground singlet, and an excited-state doublet with excitation energy Δ ($= 32$ cm^{-1} in TmES and LiTmF_4). In a magnetic field the doublet $|d_{1,2}\rangle$ is split (the magnitude of the splitting is denoted by $\hbar\Omega$). Every term involving the nuclear spin ($I = 1/2$) is twofold degenerate, and inclusion of the hyperfine and Zeeman interactions \mathcal{H}_{IJ}

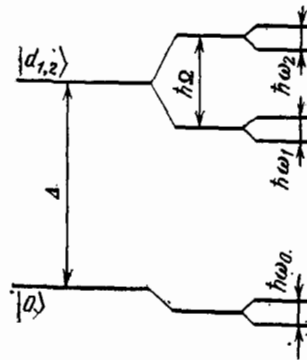


FIG. 1. Schematic model of electronic-nuclear energy levels.

and \mathcal{H}_{IZ} will lead to further splitting of the electron-nuclear states. We note that Fig. 1 recalls the sort of model spectrum investigated in the theory of nuclear magnetism, where one studies the coupling of nuclear and electronic spins (see e.g., Refs. 58, 59). This coupling is modelled by means of an artificial separation of the pairs of spins $S = 1/2$ and $I = 1/2$. In Van Vleck systems, such pairs can be separated in a natural way, and Fig. 1 can be regarded as an electron-nuclear pair spectrum with $S = 1$, $I = 1/2$, along with an initial splitting of the electronic states described by a Hamiltonian ΔS_z^2 where $\Delta > 0$.

Let us now calculate the equilibrium magnetization for one ion $\mathbf{M} = \text{Tr}(\rho \mathbf{M})$, where $\rho = \exp(-\beta_0 \mathcal{H}) / \text{Sp} \exp(-\beta_0 \mathcal{H})$ is the density matrix of the system, $\beta_0 = 1/kT$ and the magnetic moment operator is $\mathbf{M} = -g_J \mu_B \mathbf{J} + \gamma_I \hbar \mathbf{I} = \mathbf{M}_J + \mu_I$. Let us transform the expression for the average moment according to the Kubo formula⁶⁰

$$\begin{aligned} &\exp[-\beta_0 (\mathcal{H}_0 + \mathcal{H}')] \\ &= \exp(-\beta_0 \mathcal{H}_0) \left[1 - \int_0^{\beta_0} d\lambda \mathcal{H}'(\lambda) \right. \\ &\quad \left. + \int_0^{\beta_0} d\lambda_1 \int_0^{\lambda_1} d\lambda_2 \mathcal{H}'(\lambda_1) \mathcal{H}'(\lambda_2) - \dots \right], \end{aligned}$$

where $\mathcal{H}'(\lambda) = \exp(\lambda \mathcal{H}_0) \mathcal{H}' \exp(-\lambda \mathcal{H}_0) = g_J \mu_B \mathbf{HJ} \times (\lambda) + A_J \mathbf{IJ}(\lambda) - \gamma_I \hbar \mathbf{HI}$. For temperatures which are

TABLE I. Energy levels and wavefunctions of a Tm^{3+} ion in a thulium ethyl sulfate $\text{Tm}(\text{C}_2\text{H}_5\text{SO}_4)_3 \cdot 9\text{H}_2\text{O}$ crystal.⁵⁶

Energy (cm^{-1})		Wave function
Calculated*	Experiment	
300,1	302,5	$0,707 +3\rangle - 0,707 -3\rangle$
273,6	274,0	$0,895 \pm 4\rangle - 0,446 \mp 2\rangle$
221,0	—	$0,697 +6\rangle - 0,168 0\rangle + 0,697 -6\rangle$
214,8	—	$ s\rangle = 0,707 +6\rangle - 0,707 -6\rangle$
198,1	198,9	$ p_{12}\rangle = 0,953 \pm 5\rangle - 0,305 \mp 1\rangle$
157,1	157,3	$0,707 +3\rangle + 0,707 -3\rangle$
110,0	110,9	$0,446 \pm 4\rangle + 0,895 \mp 2\rangle$
31,3	32,1	$ d_{1,2}\rangle = 0,305 \pm 5\rangle + 0,953 \mp 1\rangle$
0	0	$ 0\rangle = 0,119 +6\rangle + 0,988 0\rangle + 0,119 -6\rangle$

*With crystal-field parameters $C_2^0 = 130.5$ cm^{-1} , $C_4^0 = -65.9$ cm^{-1} , $C_6^0 = -28.6$ cm^{-1} , $C_6^2 = 427.3$ cm^{-1}

not too low, i.e., $kT \gg |\mathcal{H}'|$, we can confine ourselves to the first terms of this expansion; then the electronic magnetization in first approximation is equal to

$$\mathbf{M}_H = \tilde{\chi} \mathbf{H}, \quad \chi_{\alpha\beta} = g_J^2 \mu_B^2 \int_0^{\beta_0} d\lambda \text{Tr} (\rho_0 J_\beta(\lambda) J_\alpha),$$

where ρ_0 is the density matrix for the unperturbed Hamiltonian \mathcal{H}_0 . Calculating the trace in the representation in which \mathcal{H}_0 is diagonal, we obtain in this way the Van Vleck formula for the susceptibility

$$\chi_{\alpha\beta}^T = g_J^2 \mu_B^2 \left[\sum_l \exp(-\beta_0 E_l^0) \right]^{-1} \times \sum_l [\beta_0 \langle l | J_\alpha | l' \rangle \langle l' | J_\beta | l \rangle + \langle l | J_\alpha C_l J_\beta + J_\beta C_l J_\alpha | l \rangle] \exp(-\beta_0 E_l^0); \quad (1.2)$$

Here,

$$C_l = \sum_m \frac{|m\rangle \langle m|}{E_m^0 - E_l^0}, \quad (1.3)$$

$|l\rangle, |l'\rangle$ are states whose (unperturbed) energies both equal E_l^0 . For a system with a nonmagnetic ground state, this formula is also suitable for use at very low temperatures, when only the ground state level is populated; for a ground-state singlet level, we obtain the temperature-independent susceptibility

$$\chi_{\alpha\beta}^0 = g_J^2 \mu_B^2 T_{\alpha\beta}, \quad T_{\alpha\beta} = \langle 0 | J_\alpha C_0 J_\beta + J_\beta C_0 J_\alpha | 0 \rangle. \quad (1.4)$$

The magnitude of the nuclear magnetization is in first approximation no different from the usual

$$\mathbf{m}_I^{(1)} = I(I+1) \gamma_I^2 \hbar^2 \beta_0 \mathbf{H} / 3;$$

the contribution of the second order approximation

$$\mathbf{m}_I^{(2)} = \frac{1}{3} \gamma_I \hbar A_J g_J \mu_B I (I+1) \times \int_0^{\beta_0} d\lambda_1 \int_0^{\lambda_1} d\lambda_2 \text{Tr} \{ \rho_0 [J_\beta(\lambda_1) J_\alpha(\lambda_2) + J_\alpha(\lambda_1) J_\beta(\lambda_2)] \} H_\beta,$$

may turn out to be the dominant one. A simple calculation leads to the following expression for the nuclear magnetization

$$\mathbf{m}_I = \mathbf{m}_I^{(1)} + \mathbf{m}_I^{(2)} = \frac{\gamma_I^2 \hbar^2 I (I+1)}{3kT} \left(1 + \frac{A_J}{g_J \mu_B \gamma_I \hbar} \tilde{\chi}^T \right) \mathbf{H}, \quad (1.5)$$

which corresponds to an "enhanced" external magnetic field.

The contributions in $\mathbf{M}_J = \text{Tr}(\rho \mathbf{M}_J)$ to second and third order correspond to a magnetization induced in the electronic shells by the nuclear moments. This doubly-enhanced magnetism is especially marked at very low temperatures $|\mathcal{H}'| \gg kT$. Under these conditions, the calculation of the magnetization is simplified because only the nuclear sublevels of the electronic singlet are populated. The energy and eigenfunctions of the nuclear multiplet are calculated in the following approximate manner: let us write down the electronic state to second order in the perturbation \mathcal{H}'^{61}

$$|\bar{0}\rangle = |0\rangle - P_\alpha C_0 J_\alpha |0\rangle - \frac{1}{2} |0\rangle P_\alpha P_\beta \langle 0 | J_\alpha C_0^2 J_\beta | 0 \rangle + P_\alpha P_\beta C_0 J_\alpha C_0 J_\beta |0\rangle - \gamma_I \hbar \mathbf{H} P_\alpha C_0^2 J_\alpha |0\rangle;$$

Here, $P_\alpha = g_J \mu_B H_\alpha + A_J I_\alpha$ and it is understood that repeated Greek indices are to be summed over. The electronic ground state energy of the system can in this particular approximation be viewed as an effective nuclear spin Hamiltonian

$$\langle \bar{0} | \mathcal{H}_0 + \mathcal{H}' | \bar{0} \rangle = E_0^0 - \gamma_I \hbar \mathbf{H} \mathbf{I} - g_J \mu_B A_J T_{\alpha\beta} H_\alpha I_\beta - \frac{1}{2} g_J^2 \mu_B^2 T_{\alpha\beta} H_\alpha H_\beta - \frac{1}{2} A_J^2 T_{\alpha\beta} I_\alpha I_\beta.$$

The term quadratic in field gives a common shift of all the multiplet levels; the term quadratic in the spin I , where $I = 1/2$ likewise reduces to a constant ($I_\alpha I_\beta \rightarrow 1/4 \delta_{\alpha\beta}$) and is significant only for $I > 1/2$, when it gives rise to the so-called "pseudoquadratic" correction to the nuclear quadrupole energy.⁶² For $I = 1/2$, the spin Hamiltonian can be rewritten in the following form

$$\mathcal{H}_I = -\gamma_I \hbar \left(\delta_{\alpha\beta} + \frac{A_J g_J \mu_B}{\gamma_I \hbar} T_{\alpha\beta} \right) H_\alpha I_\beta = -\gamma_I \hbar \mathbf{H} (1 + \tilde{\alpha}) \mathbf{I} = -\hbar \mathbf{H} \tilde{\gamma} \mathbf{I} = -\gamma_I \hbar \mathbf{H}' \mathbf{I}. \quad (1.6)$$

Here we introduce the paramagnetic NMR shift tensor $\tilde{\alpha}$, the effective gyromagnetic ratio tensor $\tilde{\gamma}$ and the enhanced magnetic field \mathbf{H}' . The splitting of the nuclear doublet for an arbitrary orientation of the magnetic field is equal to $\hbar \omega_0 = \gamma_I \hbar H'$, $H' = \sqrt{\mathbf{H}'^2}$, while the stationary electronic states can be written in the form

$$|\bar{0}1\rangle = N_1 |\bar{0}\rangle \left(\left| +\frac{1}{2} \right\rangle + \frac{H'_x + iH'_y}{H'_z + H'} \left| -\frac{1}{2} \right\rangle \right), \quad (1.7)$$

$$|\bar{0}2\rangle = N_2 |\bar{0}\rangle \left(\left| -\frac{1}{2} \right\rangle + \frac{H'_z - H'}{H'_x + iH'_y} \left| +\frac{1}{2} \right\rangle \right),$$

where N_1, N_2 are normalization factors. Now, neglecting entirely the fact that other electron-nuclear states excepting (1.7), are populated, we obtain after some calculation the following expressions for the magnetization:

$$\mathbf{M} = \mathbf{m}_I + \mathbf{M}_J, \quad \mathbf{M}_J = \mathbf{M}_H + \mathbf{M}_I,$$

$$\mathbf{m}_I = \frac{\gamma_I \hbar}{2} \left(1 + \frac{A_J g_J \mu_B}{\gamma_I \hbar} \tilde{T} \right) \frac{\mathbf{H}}{H'} \text{th} \frac{\gamma_I \hbar H'}{2kT}, \quad (1.8)$$

$$\mathbf{M}_H = g_J^2 \mu_B^2 \tilde{T} \mathbf{H} = \tilde{\chi}^0 \mathbf{H}, \quad (1.9)$$

$$\mathbf{M}_I = \frac{A_J g_J \mu_B}{\gamma_I \hbar} \tilde{T} \mathbf{m}_I = \frac{1}{2} A_J g_J \mu_B \tilde{T} \left(1 + \frac{A_J g_J \mu_B}{\gamma_I \hbar} \tilde{T} \right) \frac{\mathbf{H}}{H'} \text{th} \frac{\gamma_I \hbar H'}{2kT}. \quad (1.10)$$

For $kT \gg \hbar \omega_0$, as was to be expected, \mathbf{m}_I coincides with (1.5), while the direction of \mathbf{m}_I (according to (1.6) this is also the quantization axis Z of the nuclear spin, and the direction of the effective "enhanced" field \mathbf{H}') is in general different from the direction of the Van Vleck magnetization \mathbf{M}_H . Usually \mathbf{M}_H greatly exceeds all other contributions to \mathbf{M} , but, as Bleaney⁶³ has remarked, for very low temperatures when the nuclear spin system is obviously polarized even by a weak magnetic field, it is possible for \mathbf{M}_I to be the dominant term. For crystals with axial symmetry, all the components of \mathbf{M} lie in the plane containing the symmetry axis c and the magnetic field direction. Fig. 2 illustrates the "fan" of these components for thulium ethyl sulfate when

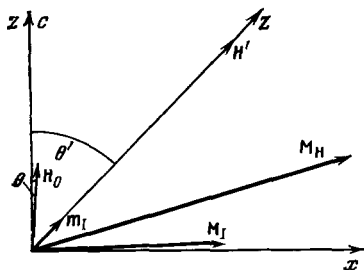


FIG. 2. Components of the magnetic moment of a $^{169}\text{Tm}^{3+}$ ion in the TmES crystal. The external magnetic field H_0 makes an angle with the crystal c axis of $\theta = 1^\circ$, while the effective (enhanced) field H' at the nucleus and the nuclear moment m_I make an angle $\theta' = 44^\circ$, the (Van Vleck) electronic moment M_H makes an angle of 74° , and the electronic-nuclear moment M_I makes an angle of 89° .

the external field is oriented at an angle of 1° to the c -axis. When the system has axial symmetry the paramagnetic shift tensor has two independent components (along the principal axes— α_{\parallel} and α_{\perp}). The part of the magnetization due to the nuclear spin, for $\hbar \omega_0 \ll kT \ll \Delta$, conforms to the usual Curie law:

$$M_{Ij} + m_{Ij} = \frac{\gamma_I^2 \hbar^2}{4kT} (1 + \alpha_j)^2 H_j,$$

which corresponds to an “enhanced” nuclear magnetic moment $\gamma_I \hbar (1 + \tilde{\alpha}) I$.

b) Distinctive features of nuclear magnetic resonance

Let us move on to a more detailed examination of the distinctive features of NMR in Van Vleck paramagnets, for the specific examples TmES and LiTmF_4 . Within the framework of the second-order perturbation theory used in section 1a) the spin Hamiltonian of the thulium nucleus can be written in the simple form

$$\begin{aligned} \mathcal{H}_I = & -\gamma_{\perp} \hbar H (I_x \sin \theta \cos \varphi + I_y \sin \theta \sin \varphi) \\ & -\gamma_{\parallel} \hbar H I_z \cos \theta, \end{aligned} \quad (1.11)$$

where θ and φ are the polar angles of the vector \mathbf{H} in the principal axis system of the tensor γ . Measurements of thulium NMR in TmEs for the temperature range 1.6° – 4.2° K show^{64,65,77} that the parameters in the spin Hamiltonian differ by more than a factor of 50:

$$\begin{aligned} \left| \frac{\gamma_{\parallel}}{2\pi} \right| &= 0.4802 \text{ (5) kHz/Oe,} \\ \left| \frac{\gamma_{\perp}}{2\pi} \right| &= 26.12 \text{ (10) kHz/Oe.} \end{aligned} \quad (1.12)$$

(in LiTmF_4 ,^{66,67} the analogous parameters equal 0.965 and 24.11 kHz/Oe respectively). Because of the extraordinarily strong anisotropy of the effective gyromagnetic ratio, fixing the orientation of the external field \mathbf{H} to lie along the c -axis of the TmES crystal is very difficult. One can see this from the angular dependence of the resonance field for a fixed-frequency spectrometer (Fig. 3). In practice, it is possible to observe the top of the peak in H_{res} for $\theta = 0$ only by dint of careful adjustment of the tilt of the cryostat in the interpolar gap of the electromagnet. Using a magnetic moment for the thulium nucleus of $-0.231 \mu_N$ ⁶² (μ_N is the nuclear magneton), we first find a gyromagnetic ratio $\gamma_I/2\pi = -0.352$

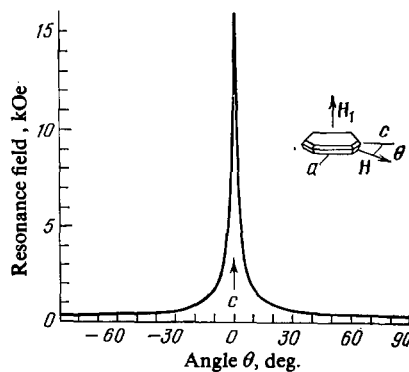


FIG. 3. Angular dependence of the resonance magnetic field for the ^{169}Tm nucleus in the TmES crystal (the temperature is 4.2°K , the resonance frequency is 7.5 MHz).

kHz/Oe, and then, using (1.6) and (1.12), the principal values of the paramagnetic NMR shift tensor at helium temperatures:

$$\alpha_{\parallel} = 0.364 \text{ (2), } \alpha_{\perp} = 73.2 \text{ (3).} \quad (1.13)$$

The reason for such strong anisotropy in the susceptibility [see (1.4) and Table I] is obvious: the longitudinal field (operator J_z) mixes into the ground state singlet $|0\rangle$ only the high-lying state $|s\rangle$, while the transverse field (operator J_x) couples $|0\rangle$ with the next excited state—the doublet $|d_{1,2}\rangle$.

We note that the corresponding transverse Van Vleck susceptibility χ_{\perp}^0 , generally speaking, depends on the orientation of the magnetic field in the plane perpendicular to the crystal c -axis. This dependence is due to the anisotropy of the electronic Zeeman interaction (a fourth-order effect which we have not allowed for), and the magnetostrictive deformation (a third order effect). Both effects are quadratic in the magnetic field, and in strong fields they are easy to detect by nonresonant methods (TmPO_4 , Ref. 68). In the weak fields we deal with here, however, this angular dependence can only be measured by the NMR method (LiTmF_4 , Ref. 69).

The test of how precisely we have aligned the orientation of \mathbf{H} along the TmES crystal c -axis is not only maximum resonance field but also minimum NMR linewidth (Fig. 4). The linewidth δH , measured in oersteds, increases monotonically with movement away from the perpendicular orientation to parallel, varying as $1/\sin\theta$; this implies that the linewidth $\delta\nu$ in frequency units remains constant with angle between 3° and 90° . In the angular interval 0 to 3° a sudden narrowing of the line occurs. This sort of angular dependence in linewidth is well known in EPR.⁷⁰ Local stress in crystals plays an important role in the EPR linewidth, leading to a spread in values of the g -tensor and “wandering” of the crystal field axes. Since the paramagnetic NMR shift is directly related to the Stark splitting of the electronic energy levels, the contribution to the NMR linewidth introduced by crystalline structural defects also plays an important role in our case. The principal cause of inhomogeneous broadening proves to be the scatter in values of the perpendicular component α_{\perp} of the line shift due to local distortion of the symmetry of the crystalline electric field.^{64,67,71–73} By virtue of

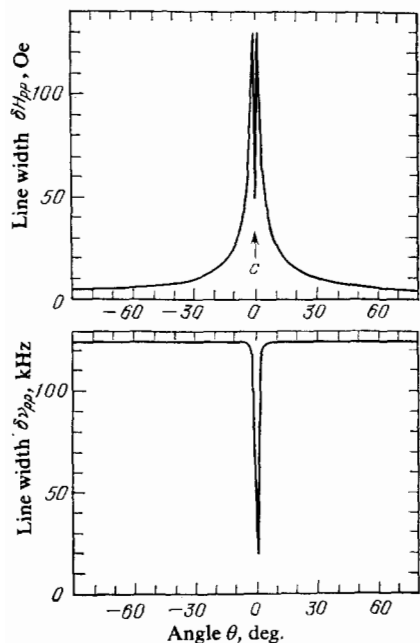


FIG. 4. Angular dependence of the resonance line width of the ^{169}Tm nucleus in TmES (the temperature is 4.2° K, the resonance frequency is 3.9 MHz).

the inequality $|\gamma_{\perp}| \gg |\gamma_{\parallel}|$, the inhomogeneous contribution to the NMR linewidth of thulium in TmES remains constant over a wide interval of the angle θ , and only when the orientation of \mathbf{H} is almost exactly parallel to the c -axis does it fall abruptly. In view of this, it is evident that the dipole linewidth must also be minimal,^{71,73} because the scatter in Larmor frequencies of the thulium nuclei is determined not only by the local fields from magnetic centers (e.g., Tm^{3+} ions, ^1H nuclei and paramagnetic impurities) but also by the magnitude of the effective gyromagnetic ratio, which is very small for $\theta = 0$. We will not enter into an in-depth analysis here of the causes of NMR line broadening (Section 2 is devoted to this); we will remark only that for low temperatures the huge electronic magnetic moments \mathbf{M}_H , which are the same in magnitude and direction for all Van Vleck ions, have absolutely no effect on the resonance line width, and that the conditions for observing various resonances in Van Vleck paramagnets (including NMR of diamagnetic atoms⁷³⁻⁷⁶ and EPR of paramagnetic impurity centers⁷⁶) are almost the same as in diamagnetic crystals.

As the temperature is increased, the crystal enters a temperature region in which rapid jumps between levels of the 4f shells become possible, and the nucleus is subjected to other rapidly-varying time-dependent hyperfine fields caused by thermal excitations of electrons. Now, in place of a single precession frequency for the nuclear spin there is a spectrum of frequencies. For sufficiently rapid changes in the electronic states a single line is observed, as before; however, this line undergoes an additional shift if the frequency spectrum under discussion is not symmetric relative to the NMR frequencies of the Van Vleck ions in the singlet state. A temperature dependence of this kind in the NMR line shift $\bar{\alpha}^T$ was observed for the first time by Jones⁴⁹ while he was investigating intermetallic compounds of praseodymium

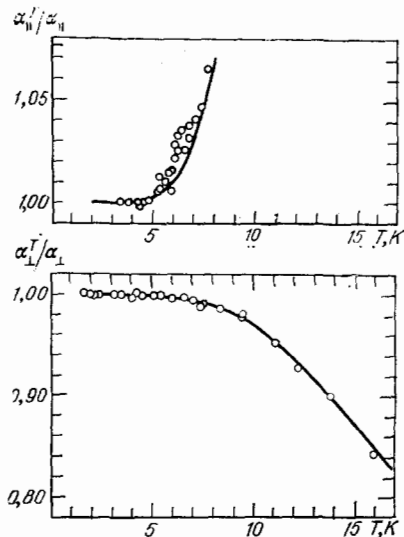


FIG. 5. Temperature dependence of the paramagnetic NMR shift of ^{169}Tm in TmES.⁷⁸ The solid curve is calculated from formula (1.2).

and thulium. Later this effect was also observed in dielectric compounds of thulium,^{64,66} praseodymium³⁶ and holmium.³⁹ In all articles in which the interpretation of experimental data is discussed, the proportionality relation $\bar{\alpha}^T \sim \chi^T$ is used, which is based on the intuitive substitution of a time averaged value for the hyperfine field on a "statistically averaged" nucleus. As experiment shows (see Fig. 5), this simple approach, under the assumption of rapid relaxation transitions between energy levels of the paramagnetic ion, ensures good results. In Sec. 3 we will give it a rigorous justification.

The temperature-dependent shift of the resonance line is inseparably bound up with the nuclear magnetic relaxation time and linewidth. While for low temperatures the linewidth is mainly determined by collective interactions, with an increase in temperature the role of intra-atomic electron-nuclear coupling becomes increasingly important. Fluctuations in the hyperfine magnetic field at the nucleus usually have components perpendicular to the external magnetic field. The Fourier spectrum of these field components contains resonance frequencies which induce transitions between nuclear energy levels, i.e., nuclear relaxation. There is a deep analogy between the situation under study here and NMR phenomena in liquids. The form $A \mathbf{J}(t) \cdot \mathbf{I}$ of the Hamiltonian for fluctuations in the hyperfine interaction attests to the presence of the peculiar "scalar relaxation of the second kind."⁵⁸ Central to the pursuit of this analogy is the question of the correlation time for the fluctuation process, which, as will be shown in Sec. 3, coincides with the life time of a Van Vleck ion in an excited electronic level.^{77,78} In magnetically "dilute" crystals the life time of an electronic excitation is usually limited by electronic-vibronic interactions, and equals the inverse of the probability for spontaneous emission of a phonon with the corresponding energy Δ . In magnetically "concentrated" crystals, however, the magnetic dipole-dipole interaction between Van Vleck ions is a significantly larger effect, thanks to which the electronic excit-

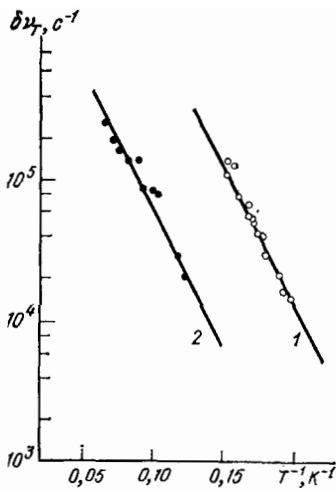


FIG. 6. Increase of the NMR line width of ^{169}Tm in TmES as a function of reciprocal temperature.^{77,78} Curve 1 is for $\mathbf{H}\parallel c$, the resonance frequency is 3.9 MHz; curve 2 is for $\mathbf{H}\perp c$, the resonance frequency is 11 MHz. The straight lines correspond to the dependence $\sim \exp(-46/T)$.

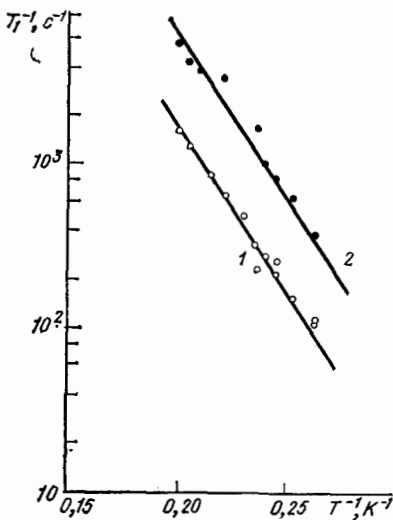


FIG. 7. Relaxation rate for longitudinal magnetization of ^{169}Tm in TmES as a function of reciprocal temperature.⁷⁹ Curve 1 is for $\mathbf{H}\parallel c$, the resonance frequency is 7.5 MHz; curve 2 is for $\mathbf{H}\perp c$, the resonance frequency is 13 MHz. The straight lines correspond to the dependence $\sim \exp(-46/T)$.

ed states are rapidly transported from one ion to another⁷⁹ (calculated estimates of the transition probability are discussed in Sec. 2).

On the basis of general ideas relating to this "scalar relaxation of the second kind,"⁵⁸ one can at once infer that the relaxation rates $1/T_1$ and $1/T_2$ will have the same temperature dependence. One can also foresee the nature of this dependence, if one notes that the corresponding correlation functions for the electronic magnetization must contain the transition probability for an ion into an excited state, i.e., a Boltzmann factor $\exp(-\Delta/kT)$. Experiment fully confirms these hypotheses: both the additional NMR linewidth (Fig. 6) and the spin-lattice relaxation rate for ^{169}Tm in TmES (Fig. 7) vary with temperature according to an exponential law with parameter $\Delta = 32 \text{ cm}^{-1}$ (46°K), precisely equal to the energy difference between the ground state and the doublet $|d_{1,2}\rangle$. In Sections 2 and 3 we will show how, given full information about the crystal structure and electronic energy spectrum, one can estimate with fair precision the magnetic relaxation rate for nuclei of Van Vleck ions. Here, however, we present only the well known experimental data for nuclear relaxation due to fluctuations of the hyperfine magnetic field (Table II).

c) Nuclear magnetic cooling

The intermediate character of magnetism in the materials we have studied naturally suggests that they be applied to the technology of magnetic cooling. The method of obtaining ultralow temperatures by means of adiabatic demagnetization of the usual paramagnetic salts has limitations connected with the comparatively high (10^{-2} – 10^{-3} °K) temperatures associated with magnetic ordering of the electronic spins. Up to recent times, the only method of obtaining temperatures below 10^{-3} °K was adiabatic demagnetization of nuclear moments in metals (for example, the nuclei ^{63}Cu and ^{65}Cu in metallic copper). In principle, nuclear cooling is no different from electronic cooling; however, for engineering feasibility it requires very strict initial conditions, specifically ratios H/T approximately 1000 times as large as those required for the latter. Because of the small values of the nuclear magnetic moments under realizable conditions, one does not succeed in making full use of the entropy (and correspondingly the cooling capacity) of the nuclear cooling stages; for example, for a temperature of 20 mK, an external field of strength 80 kOe decreases the en-

TABLE II. Experimental data on spin-lattice relaxation of ^{141}Pr and ^{169}Tm nuclei in dielectric Van Vleck paramagnets: $T_1^{-1} = A \exp(-\Delta'/kT)$.

Crystal	Temperature, °K	Orientation of magnetic field	A, sec^{-1}	Δ', cm^{-1}
$\text{Pr}_2(\text{SO}_4)_3 \cdot 8\text{H}_2\text{O}$ ³⁰	6–9,2	arbitrary	$8,4 \cdot 10^7$	55
$\text{Pr}(\text{NO}_3)_3 \cdot 6\text{H}_2\text{O}$ ³⁰	3,5–5,5		$4,0 \cdot 10^8$	27
$\text{Pr}(\text{ReO}_4)_3 \cdot 4\text{H}_2\text{O}$ ³⁰	2,5–5,2		$2,2 \cdot 10^8$	19,7
TmES ^{13, 64}	3,0–5,0	$\mathbf{H} \perp c$	$1,8 \cdot 10^8$	32
LiTmF_4 ⁷⁶	2,5–4,2	$\mathbf{H} \parallel c$	$4,4 \cdot 10^8$	27
TmPO_4 ⁴⁴	2,5–3,4	$\mathbf{H} \perp c$	$3,1 \cdot 10^8$	25,6
TmVO_4 ⁴⁴	0,3–1,0	$\mathbf{H} \parallel c$	$1,4 \cdot 10^4$	1,5

entropy of copper nuclei by only 2.1%. Therefore, the suggestion by Al'tshuler (Ref. 5) that Van Vleck paramagnets be used as nuclear refrigerants quickly found application in cryogenic engineering.^{6,7} The phenomenon of magnetic field enhancement at the nuclei of Van Vleck ions is used to produce demagnetization under less strict initial conditions than are usual for nuclear cooling: alternatively, under the latter (i.e., stricter) initial conditions one can utilize a larger fraction of the entropy of the sample. For example, the same field of 80 kOe decreases the nuclear entropy of the TmES crystal familiar to us by 2.1% already at 0.29 °K (the temperature of liquid He³), while at $T = 20$ mK this field almost removes it all (94%).

In experiments on magnetic cooling, it is important to have good heat contact between the spin system and the lattice. Therefore the highest priority was given to searching for suitable intermetallic Van Vleck compounds,⁸⁰ in which due to the presence of conduction electrons the nuclear spin-lattice relaxation time is always far shorter than in dielectrics. Selecting the compound PrNi₅, Andres and Darack⁸¹ were able to attain temperatures of 0.8 mK and cool ³He down to 1 mK. Later, Pobell and coworkers⁸² attained a temperature of 0.19 mK using the same material.

An important circumstance must be noted here which has hindered to a significant degree further progress in attaining lower temperatures. Due to the conduction electrons of intermetallic compounds of rare-earths, there is a strong s-f exchange interaction and a high magnetic ordering temperature for nuclear spins; for example, the compound PtNi₅ mentioned above has a T_c of 0.42 mK.⁸³ At the present time, RE intermetallics are most efficacious^{80,82} when used in the first (preliminary) stage of a combination "nuclear refrigerator," which uses as a second stage the traditional material copper.

In dielectric Van Vleck paramagnets, the coupling of nuclear spins with vibrations of the crystal lattice is much weaker than in the intermetallics. This keeps us from using them for cooling other materials, but does not interfere with our obtaining low temperatures for the nuclear spin system itself: for ¹⁶⁹Tm in TmVO₄, 0.1 mK,⁴⁴ for ¹⁶⁹Tm in TmPO₄, 0.4 mK,⁴⁴ for ¹⁶⁵Ho in HoVO₄, 1 mK.²⁴ It is possible, however, that these dielectrics may yet be successfully used to supercool nuclei of ³He by direct (cross-relaxation) transport of the spin temperature of Van Vleck ion nuclei through the crystal-liquid interface.⁸⁵

2. SPIN-SPIN INTERACTIONS

a) Interaction of 4f electrons with nuclei of diamagnetic ligands

Let us first examine the interaction of the 4f electron shell of a Van Vleck ion with the nuclear moments of diamagnetic atoms; we will assume that the electronic orbits of the atoms do not overlap, and that the RE ion and ligand nucleus interact as point magnetic dipoles (cf. Ref. 75). The Hamiltonian of these pairs in an external field \mathbf{H} takes the form

$$\mathcal{H} = -\gamma_1 \hbar \mathbf{H} \mathbf{I}_1 + g_J \mu_B \mathbf{H} \mathbf{J} + \mathcal{H}_{J1},$$

analogous to (1.1), but with the substitution of the dipole-dipole interaction term \mathcal{H}_{J1} for the last term. Correspondingly, the effective nuclear spin Hamiltonian of the ligands has the form $\mathcal{H}_1 = -\gamma_1 \hbar \mathbf{H} (1 + L) \mathbf{I}_1$, analogous to (1.6), where the tensor shift \tilde{L} occurs as a result of the combination of \mathcal{H}_{J1} and $g_J \mu_B \mathbf{H} \cdot \mathbf{J}$ in second-order perturbation theory. In crystals of TmES and LiTmF₄ the components of the Van Vleck susceptibility χ_{\parallel}^1 are very small; thus, the NMR spectra of the ligands in the field $\mathbf{H} \parallel c$ are of no practical interest. Let the magnetic field be perpendicular to the c -axis (z) and make an angle φ with the a -axis (x). Then the components of the shift tensor equal

$$\begin{aligned} L_x &= -\chi_{\perp}^0 (\Sigma_1 \cos \varphi - \Sigma_3 \sin \varphi), \\ L_y &= -\chi_{\perp}^0 (\Sigma_2 \sin \varphi - \Sigma_3 \cos \varphi), \\ L_z &= \chi_{\perp}^0 (\Sigma_4 \cos \varphi + \Sigma_5 \sin \varphi). \end{aligned} \quad (2.1)$$

Here

$$\begin{aligned} \Sigma_1 &= \sum_i (r_i^2 - 3x_i^2) r_i^{-5}, & \Sigma_2 &= \sum_i (r_i^2 - 3y_i^2) r_i^{-5}, \\ \Sigma_3 &= 3 \sum_i x_i y_i r_i^{-5}, & \Sigma_4 &= 3 \sum_i x_i z_i r_i^{-5}, & \Sigma_5 &= 3 \sum_i y_i z_i r_i^{-5}, \end{aligned} \quad (2.2)$$

r_i is the radius vector between the ligand and the i th Tm³⁺ ion, and the summation extends over all the Tm³⁺ ions surrounding a given nucleus. At the frequency $\omega_0 = \gamma_1 H_0$, resonance of the ligand nucleus is observed in the field

$$H_1 = H_0 \sqrt{(L_x + \cos \varphi)^2 + (L_y + \sin \varphi)^2 + L_z^2}. \quad (2.3)$$

If $|L_{\infty}| < 0.1$, then in place of (2.3) we can use the approximate formula

$$\frac{H_1}{H_0} - 1 \approx \chi_{\perp}^0 \left(\frac{\Sigma_1 + \Sigma_2}{2} - \sin 2\varphi \Sigma_3 - \cos 2\varphi \frac{\Sigma_2 - \Sigma_1}{2} \right). \quad (2.4)$$

Expressions (2.1), (2.3), and (2.4) correspond to the low-temperature case, when the Van Vleck ions are in their electronic ground states. Upon heating of the crystal, rapid relaxation transitions take place between Stark levels of the RE ions; the local field at the ligand nuclei is then "averaged out" and is found to be simply proportional to the paramagnetic susceptibility of the crystal at the given temperature.

The width ΔH of the proton magnetic resonance spectrum in the TmES crystal is at helium temperatures almost 8% of the applied magnetic field (Ref. 74). By studying the dependence of this resonance spectrum on the angle φ , one can attempt to determine the coordination of the hydrogen atoms.⁷³ In yttrium ethyl sulfate, the position of every atom in the lattice was found in Ref. 86 by the method of neutron diffraction, so that one can assume that in our case the only unknowns are the lattice parameters of TmES at liquid helium temperatures. In order to obtain the latter, it is sufficient to determine the coordinates of a few protons—for example, those which go into making up the molecules of water of crystallization. The water-of-crystallization protons [H(4), H(5A), H(5B) in the notation of Ref. 86] are nearest to the RE ion, and are subject to the action of the strongest local field; in the NMR spectrum for a field $\mathbf{H} \parallel c$, their lines always turn out to be the outermost ones. Thus, the problem reduces to selecting those lattice parameters for which the calculated

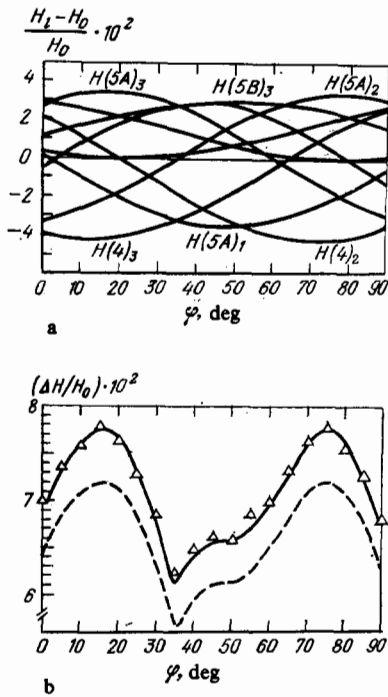


FIG. 8. Local magnetic field at protons belonging to molecules of water of crystallization (graph a), and spectral width of proton magnetic resonance (graph b), in crystals of TmES for a temperature of 4.2° K.⁷³ Solid curves—calculations using lattice parameters $a_0 = 13.59$ Å, $c_0 = 6.86$ Å; dotted curve—calculation with lattice parameters for YES.

differences of the resonance fields of the protons H(5A), H(5B) and H(4) coincide with the observed values of ΔH . Figure 8a shows the results of a calculation of the local fields at the protons of the water of crystallization, performed with the lattice parameters $a_0 = 13.59$ Å, $c_0 = 6.86$ Å. In calculating the local field at the protons using formula (2.4) a value of $\chi_1^0 = 7.07 \times 10^{-25} \text{cm}^3/\text{ion}$ was taken for the Van Vleck susceptibility of the Tm^{3+} ion obtained from measurement of the paramagnetic NMR shift of ^{169}Tm [see (1.4), (1.6), and (1.13)] using the following calculated values of the Landé g -factor and hyperfine interaction constant^{62,77}: $g_J = 1.1638$, $A_J/h = -393.5$ MHz. The good agreement between the measured and calculated spectral width (the continuous curve in Fig. 8b) lends plausibility to the chosen values of a_0 and c_0 ; for comparison, in Fig. 8b we show by a dashed line the results of an analogous calculation with the lattice parameters for YES,⁸⁶ which are only 2% higher than ours.

b) Interaction of nuclei of Van Vleck ions with one another

In the first Section, by dint of investigating the interactions of Van Vleck ions with an external magnetic field, we convinced ourselves that the nuclear magnetic moment, surrounded by the shell of 4f electrons, behaves simply as an anisotropic dipole moment $\mu = \tilde{\gamma} \tilde{I}$. The Hamiltonian for the interaction of two such dipoles in a coordinate system related to the principal axes of the axially-symmetric crystal electric field takes the form

$$\begin{aligned} \mathcal{H}_{II} = & \frac{\hbar^2}{r^3} \left[\gamma_{\perp}^2 (I_{1x} I_{2x} + I_{1y} I_{2y}) + \gamma_{\parallel}^2 I_{1z} I_{2z} \right. \\ & - \frac{3}{r^3} (\gamma_{\perp} I_{1x} x + \gamma_{\perp} I_{1y} y + \gamma_{\parallel} I_{1z} z) \\ & \left. \times (\gamma_{\perp} I_{2x} x + \gamma_{\perp} I_{2y} y + \gamma_{\parallel} I_{2z} z) \right]. \end{aligned} \quad (2.5)$$

As a result of interaction (2.5) the NMR line is broadened. In the second moment of the resonance absorption line, only the "secular" part of the dipole-dipole interaction Hamiltonian, i.e., the part which commutes with the nuclear Zeeman interaction Hamiltonian, gives any contribution. Let the external field \mathbf{H} have some arbitrary direction, which is specified in the coordinate system we have chosen by the angles θ and φ . Then the Zeeman Hamiltonian for a pair of nuclei $\mathcal{H} = \mathcal{H}_I^{(1)} + \mathcal{H}_I^{(2)}$ (see 1.11) can be transformed to diagonal form

$$\mathcal{H}_Z = -\gamma \hbar H (I_{1z} + I_{2z}), \quad \gamma = \sqrt{\gamma_{\parallel}^2 \cos^2 \theta + \gamma_{\perp}^2 \sin^2 \theta}, \quad (2.6)$$

once we have switched to the new coordinates (X, Y, Z). This transformation is effected by rotating the old coordinate system by an angle φ around the z-axis and an angle θ' around the Y-axis. The value of θ' is determined from the relation $\sin \theta' = (\gamma_{\perp}/\gamma) \sin \theta$. In the new coordinate system, the secular part of the Hamiltonian takes the form

$$\mathcal{H}_{II}^0 = \frac{\gamma^2 \hbar^2}{r^3} \left[A_{12} I_{1z} I_{2z} - \frac{B_{12}}{4} (I_{1+} I_{2-} + I_{1-} I_{2+}) \right], \quad (2.7)$$

$$\begin{aligned} \gamma^4 A_{12} = & \left(\gamma_{\parallel}^4 \cos^2 \theta - \frac{1}{2} \gamma_{\perp}^4 \sin^2 \theta \right) \left(1 - \frac{3z^2}{r^2} \right) \\ & - \frac{3}{2} \gamma_{\perp}^4 \sin^2 \theta \cos 2\varphi \cdot \frac{x^2 - y^2}{r^2} \\ & - 3\gamma_{\perp}^4 \sin^2 \theta \cdot \sin 2\varphi \cdot \frac{xy}{r^2} \\ & - 3\gamma_{\parallel}^2 \gamma_{\perp}^2 \sin 2\theta \cdot \frac{z}{r^2} (x \cos \varphi + y \sin \varphi), \end{aligned} \quad (2.7a)$$

$$\begin{aligned} \gamma^4 B_{12} = & \gamma_{\perp}^2 \left(\frac{1}{2} \gamma_{\perp}^2 \sin^2 \theta + \gamma_{\parallel}^2 \cos 2\theta \right) \left(1 - \frac{3z^2}{r^2} \right) \\ & - \frac{3}{2} \gamma_{\perp}^4 \sin^2 \theta \cos 2\varphi \cdot \frac{x^2 - y^2}{r^2} \\ & - 3\gamma_{\perp}^4 \sin^2 \theta \sin 2\varphi \cdot \frac{xy}{r^2} \\ & - 3\gamma_{\parallel}^2 \gamma_{\perp}^2 \sin 2\theta \cdot \frac{z}{r^2} (x \cos \varphi + y \sin \varphi). \end{aligned} \quad (2.7b)$$

Here, $x = x_1 - x_2$, $y = y_1 - y_2$, $z = z_1 - z_2$ are the differences of the corresponding coordinates of the RE ions. In the TmES and LiTmF₄ crystals the ratio $\gamma_{\perp}^2/\gamma_{\parallel}^2$ is very large. Thus, in a field \mathbf{H} parallel to the c -axis of the crystal, $B_{12} \gg A_{12}$, and so the interaction of the enhanced magnetic moments of the thulium nuclei are essentially purely diamagnetic in character.

The second moment of the NMR line of ^{169}Tm , which is broadened due to the interaction (2.7), is calculated in the usual way (Ref. 58):

$$M_2^{(II)} = \frac{1}{3} I(I+1) \gamma^4 \hbar^2 \sum_j r_j^{-6} \left(A_{1j} + \frac{1}{2} B_{1j} \right)^2. \quad (2.8)$$

Substituting (2.7a) and (2.7b) into (2.8), and transforming the latter (taking into account the usual considerations of

symmetry) yields for the tetragonal LiTmF₄ crystal⁷¹

$$M_{\parallel}^{(II)} [\text{rad}^2/\text{sec}^2] = \frac{\hbar^2}{4\gamma^4} \left[\frac{1}{16} (2\gamma_{\parallel}^2 + \gamma_{\perp}^2)^2 \right. \\ \times (2\gamma_{\parallel}^2 \cos^2 \theta - \gamma_{\perp}^2 \sin^2 \theta)^2 \Sigma_6 \\ + \frac{81}{8} \gamma_{\parallel}^4 \gamma_{\perp}^4 \sin^2 2\theta \Sigma_7 \\ \left. + \frac{81}{32} \gamma_{\perp}^8 \sin^4 \theta (\Sigma_8 + \cos 4\varphi \Sigma_9) \right]. \quad (2.9)$$

Here

$$\Sigma_6 = \sum_j (r_j^2 - 3z_j^2)^2 r_j^{-10}, \quad \Sigma_7 = \sum_j z_j^2 (x_j^2 + y_j^2) r_j^{-10}, \\ \Sigma_8 = \sum_j (x_j^2 + y_j^2)^2 r_j^{-10}, \quad \Sigma_9 = \sum_j (x_j^4 - 6x_j^2 y_j^2 + y_j^4) r_j^{-10}. \quad (2.10)$$

For crystals of trigonal symmetry like TmES, $\Sigma_9 = 0$. If the external field \mathbf{H} is directed along the c -axis, then for both crystals we have

$$M_{\parallel}^{(II)} = \frac{1}{16} \hbar^2 (2\gamma_{\parallel}^2 + \gamma_{\perp}^2)^2 \Sigma_6. \quad (2.11)$$

c) Interaction of nuclei of Van Vleck ions with diamagnetic ligand nuclei and with paramagnetic impurity ions

The secular part of the dipole-dipole interaction Hamiltonian for the various sorts of spins contains, as is well-known, only the operator $I_{1z} I_{2z}$. The quantization axes for spin 1 (the RE ion nucleus) and spin 2 (the ligand nucleus) are different; the direction of the z' -axis (Z) is determined as in (2.6), while the z'' -axis is in fact directed along the field \mathbf{H} (see Sec. 2a). By means of simple transformations, the secular part of the nuclear interaction Hamiltonian between the RE ion and the ligand can be put into the form

$$\mathcal{H}_{1l}^0 = I_{1z} I_{2z} \frac{\gamma_l \hbar^2}{\gamma r^3} \left[\left(\gamma_{\parallel}^2 \cos^2 \theta - \frac{1}{2} \gamma_{\perp}^2 \sin^2 \theta \right) \left(1 - \frac{3z^2}{r^2} \right) \right. \\ - \frac{3}{2} \gamma_{\perp}^2 \sin^2 \theta \cos 2\varphi \cdot \frac{x^2 - y^2}{r^2} \\ - 3\gamma_{\perp}^2 \sin^2 \theta \sin 2\varphi \cdot \frac{xy}{r^2} \\ \left. - \frac{3}{2} (\gamma_{\parallel}^2 + \gamma_{\perp}^2) \sin 2\theta \cdot \frac{z}{r^2} (x \cos \varphi + y \sin \varphi) \right].$$

The principal consequence of the interaction between the nuclear moments of Van Vleck ions and the ligand nuclei is inhomogeneous broadening of the resonance lines. The corresponding contribution to the second moment of the NMR line for ¹⁶⁹Tm in crystals of LiTmF₄ type equals⁷¹

$$M_{\parallel}^{(II)} = \frac{1}{3} I_l (I_l + 1) \frac{\gamma_l^2 \hbar^2}{\gamma^2} \left[\frac{1}{4} (2\gamma_{\parallel}^2 \cos^2 \theta - \gamma_{\perp}^2 \sin^2 \theta)^2 \Sigma_6 \right. \\ + \frac{9}{8} (\gamma_{\parallel}^2 + \gamma_{\perp}^2)^2 \sin^2 2\theta \Sigma_7 \\ \left. + \frac{9}{8} \gamma_{\perp}^4 \sin^4 \theta (\Sigma_8 + \cos 4\varphi \Sigma_9 + 4 \sin 4\varphi \Sigma_{10}) \right]. \quad (2.13)$$

For the TmES crystal, which has trigonal symmetry, $\Sigma_9 = \Sigma_{10} = 0$. Into formula (2.13) we insert the sum

$$\Sigma_{10} = \sum_j x_j y_j (x_j^2 - y_j^2) r_j^{-10}. \quad (2.14)$$

The contribution from ligands to the second moment of the NMR line in a field $\mathbf{H} \parallel c$ is proportional to γ_{\parallel}^2 , and in the TmES and LiTmF₄ crystals turns out to be negligibly small.

We now turn to paramagnetic impurity ions. If S is the effective spin of the impurity center, and g_{\parallel}, g_{\perp} are the principal components of the g -tensor, then the secular part of the I - S dipole-dipole interaction Hamiltonian in a coordinate system tied to the crystal axes takes the form

$$\mathcal{H}_{IS}^0 = I_z S_z'' \frac{\hbar \mu_B}{g \gamma r^3} \left\{ \left(\frac{1}{2} g_{\perp}^2 \gamma_{\perp}^2 \sin^2 \theta - g_{\parallel}^2 \gamma_{\parallel}^2 \cos^2 \theta \right) \left(1 - \frac{3z^2}{r^2} \right) \right. \\ + \frac{3}{2} g_{\perp}^2 \gamma_{\perp}^2 \sin^2 \theta \cos 2\varphi \cdot \frac{x^2 - y^2}{r^2} \\ + 3g_{\perp}^2 \gamma_{\perp}^2 \sin^2 \theta \sin 2\varphi \cdot \frac{xy}{r^2} \\ \left. + \frac{3}{2} (g_{\parallel}^2 \gamma_{\perp}^2 + g_{\perp}^2 \gamma_{\parallel}^2) \sin 2\theta \cdot \frac{z}{r^2} (x \cos \varphi + y \sin \varphi) \right\}. \quad (2.15)$$

Here, $g = \sqrt{g_{\parallel}^2 \cos^2 \theta + g_{\perp}^2 \sin^2 \theta}$, and the direction of z'' , i.e., the quantization axis of the electron spin S , is fixed by the polar angles φ and $\theta_S = \arctan[(g_{\perp}/g_{\parallel}) \tan \theta]$. The impurity spins are distributed over the sites of the crystal lattice in a random fashion, and so in calculating the contribution of $M_{\parallel}^{(IS)}$ to the second moment of the NMR line shape of a Van Vleck ion there arises the question of how to perform the lattice sum. Nearest-neighbor spins produce local fields which are so strong that their NMR frequencies lie far outside the limits of observed resonance linewidths. Therefore, it is necessary to exclude the corresponding terms from the sum (2.10). The indeterminateness of this "truncation" procedure can be eliminated by empirical means. To do this, we have adopted the following procedure: in $\Sigma_6 \div \Sigma_9$ we retain the terms with $r_j > R_S$, choosing R_S to be the distance at which a spin S creates a local field twice as big as the observed NMR linewidths of Van Vleck ions. Then the expression for the second moment of the NMR line shape takes the form⁷³:

$$M_{\parallel}^{(IS)} = f_S \cdot \frac{1}{3} S(S+1) \\ \times \frac{\mu_B^2}{g^2 \gamma^2} \left[\left(\frac{1}{2} g_{\perp}^2 \gamma_{\perp}^2 \sin^2 \theta - g_{\parallel}^2 \gamma_{\parallel}^2 \cos^2 \theta \right)^2 \Sigma_6^S \right. \\ + \frac{9}{8} (g_{\parallel}^2 \gamma_{\perp}^2 + g_{\perp}^2 \gamma_{\parallel}^2)^2 \sin^2 2\theta \Sigma_7^S \\ \left. + \frac{9}{8} g_{\perp}^4 \gamma_{\perp}^4 \sin^4 \theta (\Sigma_8^S + \cos 4\varphi \Sigma_9^S) \right]. \quad (2.16)$$

d) Nuclear resonance line broadening of Van Vleck ions

Knowing the atomic coordination for crystals of RE ethyl sulfates⁸⁶ and the lattice parameters for TmES at low temperatures (see Sec. 2a) it is possible for us to calculate the various contributions to the second moment of the NMR line for ¹⁶⁹Tm, and by means of a comparison of the calculated values of M_2 with measured ones, to establish the principal causes of resonance line broadening in real crystals. Results of calculations and experiment⁷³ are shown in Fig. 9. Contributions to the second moment due to interaction of the ¹⁶⁹Tm nuclei with one another (curve 1) and with ¹H nuclei (curve 2) were calculated using formulae (2.9) and

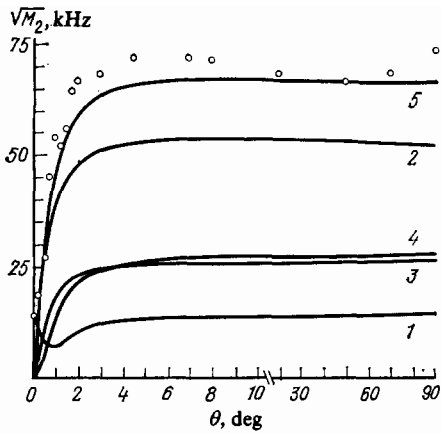


FIG. 9. Angular dependence of the second moment of the NMR line of ^{169}Tm in TmES .⁷³ The temperature is 4.2 °K, the resonance frequency is 3.9 MHz (see text for clarification).

(2.13) with the following values inserted into their lattice sums (in units of 10^{44} cm^{-6} : $\Sigma_6^{\text{Tm}} = 0.862$, $\Sigma_7^{\text{Tm}} = 0.028$, $\Sigma_8^{\text{Tm}} = 0.138$, $\Sigma_6^{\text{H}} = 136.9$, $\Sigma_7^{\text{H}} = 48.2$, $\Sigma_8^{\text{H}} = 147.2$. According to EPR data, the crystal under study contained impurity atoms of Tb^{3+} ($f = 4.6 \times 10^{-4}$), Er^{3+} ($f = 4.6 \times 10^{-4}$) and Yb^{3+} ($f = 1.5 \times 10^{-4}$). Ions of Tb^{3+} in ethyl sulfate have the highest magnetic moments ($g_{\parallel} = 17.72$, $g_{\perp} = 0$ (cf. Ref. 62), and so their effect on the NMR linewidth of thulium is very noticeable. An investigation directed specifically at the dependence of $M_2^{(JS)}$ on the concentration of the impurity Tb^{3+} showed that formula (2.16) is correct if in the lattice sum we discard terms with $r_j < R_S = 20 \text{ \AA}$. The contribution from Tb^{3+} ions to the second moment is shown by curve 3 of Fig. 9. When making estimates of the various contributions to the second moment of the thulium NMR line, we must not neglect inhomogeneous broadening of the line. A distinctive feature of the non-dipole part of M_2 , which is a result of local distortion of the crystal field symmetry, is its quadratic dependence on the resonance frequency:

$$M_2^{\alpha} = \omega_0^2 [(1 + \alpha_{\parallel})^2 \cos^2 \theta + (1 + \alpha_{\perp})^2 \sin^2 \theta]^{-2} \\ \times \{ (1 + \alpha_{\parallel})^2 \cos^4 \theta \langle \delta \alpha_{\parallel}^2 \rangle + (1 + \alpha_{\perp})^2 \sin^4 \theta \langle \delta \alpha_{\perp}^2 \rangle \\ + [(1 + \alpha_{\perp})^2 - (1 + \alpha_{\parallel})^2] \sin^2 \theta \cos^2 \theta \langle \delta \theta^2 \rangle \}.$$

The first and second terms in the curly brackets are due to scatter in the values of the paramagnetic NMR shift of thulium, while the third is from "wandering" of the c -axis. Studies of the frequency and angular dependences of M_2 show that principal cause of inhomogeneous NMR line broadening of thulium in crystals such as LiTmF_4 and TmES was scatter in values of the perpendicular component of the paramagnetic shift α_{\perp} . In particular, for a crystal of TmES , which was measured in Ref. 73 at frequencies from 3 to 150 MHz, the value of $\langle \delta \alpha_{\perp}^2 \rangle / (1 + \alpha_{\perp})^2$ was found to be 4.8×10^{-5} . The corresponding nondipole contribution is shown in curve 4 of Fig. 9. Adding all four of these contributions to M_2 , we obtain finally curve 5, which is in fairly good agreement with experimental results. The rather small deviation ($\sim 500 \text{ kHz}^2$ for angles $\theta > 2^\circ$) can be related to the paramagnetic impurities erbium and ytterbium.

The quantitative analysis we have carried out makes it possible to understand the origin of the surprisingly strong anisotropy of the second moment of the thulium NMR line. The small value of M_2 in a field $\mathbf{H} \parallel c$ is a result of the "switching-off" of all the sources of line broadening other than the dipole-dipole interactions of thulium nuclei with one another by virtue of the inequality $|\gamma_{\parallel}| \ll |\gamma_{\perp}|$. The magnitude of M_2 in the field $\mathbf{H} \perp c$ at a frequency of 3.9 MHz is computed in the following manner: in percentages, the interaction of thulium nuclei with one another makes up 4% of the measured value of M_2 , the "thulium-proton" interaction makes up 56%, the "thulium-paramagnetic impurities (Er and Tb) interaction" makes up 25%, and interaction with defects in the crystal structure makes up 15%. A large part of the linewidth is due to scatter in the local magnetic field coming from the protons. This scatter is so large that spin echo of thulium nuclei can be observed in a homogeneous external field.^{13,64,73} The signal echo at 7–15 MHz can be described by an exponential function $v(t) \sim \exp[-(t/T_2^*)^{1.9}]$, which is close to a Gaussian ($T^* = 4$ microseconds). The Fourier transform of this signal echo (the dashed curve in Fig. 10) almost coincides with the distribution function of the resonance frequencies of thulium nuclei in the local fields of the protons. To calculate this distribution function, we confine ourselves to one molecule of ethyl sulfate, that is half of a unit cell. The local fields $h_i = \gamma_P \hbar (r_i^2 - 3x_i^2) / 2r_i^5$, created by the thirty-three protons at the thulium nucleus, are distributed within an interval from 0.85 Oe (H_2O) to 0.06 Oe (CH_3). After summation, the total local field equals $h_{\Sigma} = \pm h_1 \pm h_2 \pm \dots \pm h_{33}$. In the high-temperature approximation ($\gamma_{\perp} \hbar H \ll kT$), the + and - signs are equally probable. Fixing them in some random fashion, it is not hard to find the distribution of magnitudes of h_{Σ} and consequently the distribution of resonance frequencies. The results of calculations given in Ref. 73, in which 2000 sign combinations were included, are depicted by the dashed line in Fig. 10. As is clear, it agrees well with experiments on pulsed NMR.

e) Transport of thermally excited 4f electron states

We have investigated spin-spin interactions in Van Vleck paramagnetic crystals, along with the experimental

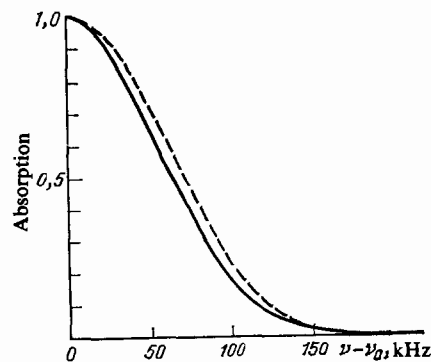


FIG. 10. Fourier transform of the spin echo signal of ^{169}Tm nuclei in TmES in a homogeneous external field $\mathbf{H} \perp c$. The resonance frequency is 13 MHz. The dashed line is the distribution function for resonance frequencies in the local fields of the nearest protons.

manifestations of these interactions, at low temperatures when only the lowest 4f electronic energy levels are populated. With an increase in temperature, the excited energy levels become populated according to the Boltzmann distribution. The 4f electrons now spend part of their time in excited states, and during this time interval the nucleus of the paramagnetic ion is exposed to the influence of other nuclei according to the strength of their hyperfine fields. In the third Section we will discuss in detail the consequences of such fluctuations in the hyperfine field; here we will only attempt to answer the question: how long is the lifetime of a state of the 4f electron shell with a given energy Δ ?

We can assume that the lifetime of an excitation is limited by spin-lattice relaxation processes, and can be determined from the inverse of the transition probability w_i for spontaneous emission of a phonon with energy Δ . For an estimate of the magnitude of w_i , we turn to the experimental data on electron spin-lattice relaxation of Ce^{3+} , Pr^{3+} , Nd^{3+} , Sm^{3+} ions in crystals of LaCl_3 , LaMgN , LaES .⁸⁷ In these crystals, the nearest excited levels of the 4f electrons differ from the ground state doublets by an interval of $\Delta = 44\text{--}48^\circ\text{K}$, while the magnitudes of the pre-exponential factor (w_i) in the two-phonon relaxation rates—which are typical of resonance fluorescence rates—vary from ion to ion but cannot exceed a limit of 6×10^8 to $4 \times 10^9 \text{ sec}^{-1}$. Thus, on the average the probability of spontaneous emission of a phonon of energy 46°K equals $2 \times 10^9 \text{ sec}^{-1}$ which corresponds to a lifetime of $\tau \approx 5 \times 10^{-10} \text{ sec}$ for an electronic excitation.

However, this estimate for the lifetime of an electronic excitation is inadequate for the case of concentrated magnetic crystals, in which the Van Vleck ions are separated by rather small distances and are coupled by strong dipole-dipole interactions (or in intermetallic compounds, by exchange). Let us show that these powerful spin-spin relaxation mechanisms reduce the lifetime by approximately an order of magnitude compared to what we obtained earlier. Let \mathcal{H}_{1l} be the dipole-dipole interaction Hamiltonian for an ion with an l th neighbor, where m and n are excited states $\psi_1 = p_1 |d_1\rangle + q_1 |d_2\rangle$, $\psi_2 = p_2 |d_1\rangle + q_2 |d_2\rangle$

$$(2.17)$$

of the ion and its neighbor, respectively. Then the "departure rate" for the excitation from the ion is written in the form

$$\frac{1}{\tau} = \frac{2\pi}{\hbar^2} \sum_{l, n} |(\mathcal{H}_{1l})_{mn}|^2 g(\omega_{mn}). \quad (2.18)$$

Here, $g(\omega)$ is a form factor, which for definiteness we choose to be a Lorentzian function

$$g(\omega) = \frac{1}{\pi} \frac{\tau}{1 + \omega^2 \tau^2}, \quad (2.19)$$

ω_{mn} is the frequency difference between the excited states m and n , equal to 0 and Ω for the two possible values of n in the sum (2.18). We introduce the notation:

$$\frac{2}{\hbar^2} \sum_l |(\mathcal{H}_{1l})_{mn}|^2 = \frac{1}{\tau_0^2} \quad (2.20)$$

and rewrite (2.18) in the form

$$\frac{1}{\tau^2} = \frac{1}{\tau_0^2} \left(1 + \frac{\kappa}{1 + \Omega^2 \tau^2} \right). \quad (2.21)$$

The first term in (2.21) corresponds to transitions of the type $\psi_1^{(1)} \rightarrow \psi_1^{(l)}, \psi_2^{(1)} \rightarrow \psi_2^{(l)}$, caused by the interaction

$$\hat{B} = -\frac{1}{4} \frac{g_j^2 \mu_B^2}{r_l^3} (1 - 3 \cos^2 \theta_l) (J_+^{(1)} J_-^{(l)} + J_-^{(1)} J_+^{(l)}). \quad (2.22)$$

Since this process occurs with conservation of the excitation energy ($\Delta + \hbar \Omega/2$, or $\Delta - \hbar \Omega/2$), the frequency difference in (2.18) is zero. The second term in (2.21) is due to the transitions $\psi_1^{(1)} \rightarrow \psi_2^{(l)}, \psi_2^{(1)} \rightarrow \psi_1^{(l)}$ which are accompanied by a change in excitation energy of magnitude $\pm \hbar \Omega$. The matrix elements of the corresponding operator

$$\hat{E} + \hat{F} = -\frac{3}{4} \frac{g_j^2 \mu_B^2}{r_l^3} \sin^2 \theta_l (e^{-2i\varphi_l} J_+^{(1)} J_+^{(l)} + e^{2i\varphi_l} J_-^{(1)} J_-^{(l)}) \quad (2.23)$$

in the general case differ from the matrix elements of (2.22); therefore, in (2.21) $\kappa \neq 1$. Let us turn again to the TmES crystal, in which the excitation energy of the doublet is exactly equal to 46°K . Transitions of the first type occur here, for the most part, due to the two nearest neighbors of the Tm^{3+} ion ($r_l = 7 \text{ \AA}, \theta_l = 0, \pi$), while transitions of the second type are due to the six neighbors on the next coordination sphere ($r_l = 8.7 \text{ \AA}, \theta_l = 66^\circ, 114^\circ$), so that $\kappa \approx 1$, $\tau_0 = 8 \times 10^{-11} \text{ sec}$, and for a constant external magnetic field oriented perpendicular to the c -axis of the crystal the lifetime of an ion in an excited state equals $5 \times 10^{-11} \text{ sec}$.

It is obvious that such an estimate of the transport time of an electronic excitation suffers from excessive oversimplification. In practice one would have to take into account successively all the interparticle interactions and the spread of energy levels of neighboring ions as a consequence of structural defects in a real crystal. This could give rise to a still larger reduction in the magnitude of τ , and a change in the relation between the form-factors and the transition probabilities for the various processes. It is important to emphasize, however, that even an approximate estimate gives us a very short lifetime for an ion in an excited state, which (through $\hbar \Omega$) depends on the crystal orientation in the magnetic field. Electronic excitations are also responsible for the very peculiar kinetics of the nuclear spins.

3. NUCLEAR MAGNETIC RELAXATION

Because the excited electronic energy levels of an ion are situated comparatively close to the ground state, they are noticeably populated even at helium temperatures, so one might expect that lines should appear in the NMR spectrum at frequencies corresponding to hyperfine fields due to excited states. In fact, however, the population determines not only the fraction of excited ions at a given moment of time, but also the average time that a particular ion spends in an excited state. In other words, the electronic state of an ion fluctuates, so the nucleus is subjected to a random interaction which makes the hyperfine field change with time; hence, the resonance spectrum depends essentially on the fluctuation rate. In the general case, the effective magnetic field at the nucleus in the presence of fluctuations varies both in magnitude and direction. If in addition to this we note that

the excited electronic states are often not singlets but magnetic doublets, then a full theory of resonance absorption appears to be hopelessly complicated. There are, however, two decisive aspects of this situation which simplify the theoretical interpretation of the experimental data on nuclear magnetic relaxation in Van Vleck paramagnets: the shortness of the correlation time of fluctuations compared to the inverse resonance frequency, and the relative smallness of the population of excited electronic states in the temperature interval in which resonance is observed.

a) Resonance lineshapes under adiabatic conditions⁷⁷

If the external magnetic field is parallel to the crystal c -axis, then as soon as a change of the electronic states of the rare-earth ions takes place, the magnitudes of the effective magnetic fields at their nuclei also change, giving rise to a jump in the NMR frequency. Therefore it is advantageous at this point to use a variant of the adiabatic theory of motional narrowing of resonance lines, which is based on a model of random variation of the resonance frequency.⁵⁸ Let the resonance frequency take on the values $\omega_0, \omega_1, \omega_2, \dots$ with probabilities W_0, W_1, W_2, \dots ; correspondingly, let π_{mn} be the transition probability per unit time for a spin to go from a state of frequency ω_m to one of frequency ω_n ; let $-\pi_{nn}$ be the probability of departure of a spin from the n th state. These probabilities conform to the obvious relations

$$\sum_n \pi_{mn} = 0, \quad W_m \pi_{mn} = W_n \pi_{nm}. \quad (3.1)$$

In the problem under discussion here, W_m is the Boltzmann factor for the various electronic states, π_{mn} is the transition probability between these states, and $-\pi_{nn}^{-1}$ is the lifetime of the n th state. If quantities related to the ground state singlet were denoted by the subscript 0 , then for temperatures much smaller than the excitation energies we have $W_0 \gg W_1, W_2, \dots$.

The resonance line shape is given by the expression $I(\omega) = \text{Re}(\mathbf{W}\mathbf{A}^{-1}\mathbf{1})$, where $\mathbf{W} = (W_0, W_1, \dots)$, $\mathbf{1}$ is a column vector all of whose elements are 1 , and the matrix \mathbf{A}^{-1} is the inverse of the matrix $A_{mn} = i(\omega_m - \omega) \delta_{mn} + \pi_{mn}$. When two frequencies are present, the line shape function takes the fairly simple form:¹⁾

$$I(\omega) = \frac{W_0 W_1 (\omega_1 - \omega_0)^2 (\pi_{00} + \pi_{11})}{(\omega_0 - \omega)^2 (\omega_1 - \omega)^2 + [\pi_{00} (\omega_1 - \omega) + \pi_{11} (\omega_0 - \omega)]^2}. \quad (3.2)$$

This lineshape function illustrates in a standard way the merging of two resonance lines with frequencies ω_0 and ω_1 as the transition rate between the two frequencies increases, and the confluence of the lines into a single one centered around an intermediate frequency when

$$\pi_{10} = \pi_{01} \gg |\omega_0 - \omega_1|.$$

The case $W_0 \neq W_1$, and correspondingly $\pi_{01} \neq \pi_{10}$, has been investigated in the book by Burshtein, for example (Ref. 88). It is very significant that the correlation time of the random process, which equals

$$\tau_c = (\pi_{10} + \pi_{01})^{-1}, \quad (3.3)$$

is determined in this case by the largest transition rate, i.e.,

the smaller of the lifetimes of the two states. For $W_0 \gg W_1$, the principal maximum of the function (3.2) is always found in the vicinity of ω_0 , regardless of the relationship between $\Delta\omega_1 = \omega_1 - \omega_0$ and τ_c^{-1} ; in this case, the function reduces to the Lorentzian function:

$$I(\omega) \approx W_1 \frac{\Gamma}{(\omega_0 - \omega + \delta\omega)^2 + \Gamma^2}, \quad (3.4)$$

where

$$\delta\omega = \frac{\Delta\omega_1 \pi_{00} (\pi_{00} + \pi_{11})}{\Delta\omega_1^2 + (\pi_{00} + \pi_{11})^2}, \quad \Gamma = \frac{|\pi_{00}| \Delta\omega_1^2}{\Delta\omega_1^2 + (\pi_{00} + \pi_{11})^2}. \quad (3.5)$$

In the case of three electronic energy levels, the function for the line shape also has the form (3.4) if it is assumed that transitions between excited states have low probability, i.e., $\pi_{12}, \pi_{21} \approx 0$ and consequently that $-\pi_{22} = \pi_{20}, -\pi_{11} = \pi_{10}$. We remark that this condition will always be fulfilled if the two excited states correspond to a magnetic doublet, as in the case of LiTmF_4 or of TmES . Actually, the probability of a spin-lattice transition between nearly degenerate levels is small when such transitions are caused by low-frequency phonons, due to the small spectral density of the latter; in addition, transitions due to dipole-dipole interactions between neighbors are to first order forbidden. The line shift and its width are determined by the formulae

$$\delta\omega = \frac{\pi_{01}\pi_{10} \Delta\omega_1}{\Delta\omega_1^2 + \pi_{10}^2} + \frac{\pi_{02}\pi_{20} \Delta\omega_2}{\Delta\omega_2^2 + \pi_{20}^2}, \quad (3.6)$$

$$\Gamma = \frac{\pi_{01} \Delta\omega_1^2}{\Delta\omega_1^2 + \pi_{10}^2} + \frac{\pi_{02} \Delta\omega_2^2}{\Delta\omega_2^2 + \pi_{20}^2},$$

which are natural generalizations of (3.5).

Turning now to the problem of the temperature dependence of the NMR frequency, we note that a simple proportionality relation between the line shift and the paramagnetic susceptibility follows from Eq. (3.6) under the condition $\pi_{m0} \gg |\Delta\omega_m|$. Then taking into account (3.1), it also follows from (3.6) that

$$\omega_{\text{res}} = \omega_0 + \Delta\omega_1 \frac{\pi_{01}}{\pi_{10}} + \Delta\omega_2 \frac{\pi_{02}}{\pi_{20}} \approx W_0 \omega_0 + W_1 \omega_1 + W_2 \omega_2,$$

i.e., the observed resonance frequency is a weighted average of all the electronic frequencies, with Boltzmann weighting factors. As long as

$$\omega_i = \gamma_I H - \frac{A_J}{\hbar} \langle J_z \rangle, \quad (3.7)$$

where the brackets signify an average over the corresponding electronic states, the resonance frequency can be expressed in terms of the susceptibility [see (1.6)]:

$$\omega_{\text{res}} = \gamma_I H \left(1 + \frac{A_J}{\gamma_I \hbar g_J \mu_B} \chi_{zz} \right). \quad (3.8)$$

It is clear that for this relation to hold, a comparatively large transition rate is required out of the excited electronic levels only.

As an example, let us examine the temperature dependence of the NMR line shift and broadening of ^{169}Tm in the TmES crystal. Confirming to our exposition of the theory discussed above, we attach to the electron states $|0\rangle, |d_1\rangle$ and $|d_2\rangle$ under investigation (see Fig. 1) the indices 0, 1 and 2, respectively. Only these three states of the $4f$ electron shell are involved in determining the temperature variation of the

thulium line width and NMR frequency. The remaining electronic levels lie far higher ($> 100 \text{ cm}^{-1}$), and the likelihood of their being populated can be neglected. For calculating the frequencies ω_i from formula (3.7), the singlet and doublet wave functions must be chosen correct to linear order in the magnetic field terms; this is not difficult to do, using the information in Table I. As a result, we obtain

$$\omega_1 - \omega_0 = \Delta\omega + \eta, \quad \omega_2 - \omega_0 = -\Delta\omega + \eta, \quad (3.9)$$

where

$$\Delta\omega = \frac{A_J}{\hbar} \langle d_2 | J_z | d_2 \rangle,$$

$$\eta = \frac{2A_J g_J \mu_B H}{\hbar} \left(\frac{\langle p | J_z | d \rangle^2}{E_p - E_d} - \frac{\langle 0 | J_z | s \rangle^2}{E_s - E_0} \right),$$

and we denote by $|s\rangle$ and $|p_{1,2}\rangle$ the states mixed into $|0\rangle$ and $|d_{1,2}\rangle$ by the magnetic field. Inserting once again the probability of relaxation transitions in formula (3.6):

$$\pi_{10} \approx \pi_{20} = \tau^{-1} \approx \tau_c^{-1}, \quad \pi_{01} = \tau^{-1} \exp\left(-\frac{\Delta}{kT}\right), \\ \pi_{02} = \tau^{-1} \exp\left(-\frac{\Delta + \hbar\Omega}{kT}\right), \quad (3.10)$$

we find for $\hbar\Omega \ll kT \ll \Delta$ that

$$\delta\omega = \frac{2\eta + \Delta\omega(\hbar\Omega/kT)\bar{i}}{1 + \Delta\omega^2\tau^2} \exp\left(-\frac{\Delta}{kT}\right), \\ \Gamma = \frac{2\Delta\omega^2\tau}{1 + \Delta\omega^2\tau^2} \exp\left(-\frac{\Delta}{kT}\right). \quad (3.11)$$

For the case of rapid fluctuations, $\Delta\omega\tau \ll 1$, and there are no longer any adjustable parameters in the formula for the line shift. Inserting the calculated magnitudes of the matrix elements, along with the values of the Landé g -factor (the calculation of which was presented earlier) and hyperfine-interaction constants of the free ion, we obtain the temperature shift parameter of the nuclear spin Hamiltonian:

$$\delta\alpha_{\parallel} = \frac{\delta\omega}{\delta_I H} = \left(3,3 + \frac{34,3}{T}\right) \exp\left(-\frac{46}{T}\right). \quad (3.12)$$

As for the line broadening, the increase which one measures experimentally is connected with the quantity Γ in the Lorentz function by the simple relation $\delta\nu_T = \Gamma/\pi\sqrt{3}$. In Figs. 11 and 6, we present results of measurement of the temperature variation of the paramagnetic shift and broadening of the NMR line of ^{169}Tm in thulium ethyl sulfate for a magnetic field oriented parallel to the crystal c -axis. The calculated curve for the shift, obtained from formula (3.12), is in fairly good agreement with experiment. This is an indication that in the case studied here the rapid-fluctuation condition is indeed realized. The line broadening obtained from theory is in good agreement with experiment (Fig. 6, line 1), if we use for the correlation time the value $\tau_c = 3.4 \times 10^{-10}$ sec, which does not violate the rapid-fluctuation condition. Within the temperature region under investigation, the role of the correlation time is played by the inverse transition probability (in units of time) from excited electronic states to the ground state. As we have already explained earlier, the rather large value of this transition probability is guaranteed by the dipole-dipole interaction between the rare-earth ions,

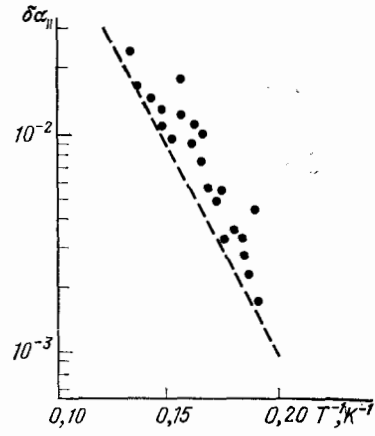


FIG. 11. Increase of the paramagnetic shift of the NMR line of ^{169}Tm in TmES as a function of reciprocal temperature,^{77,78} for a field $\mathbf{H} \parallel c$. Dashed line: the results of a calculation using formula (3.12).

although one should not overlook the electron-vibronic interaction. The smallness of the correlation time for the random process which represents the variation of the magnetic field at the nucleus allows one to proceed to an investigation of nuclear relaxation for arbitrary orientations of the external magnetic field.

b) Relaxation of nuclei of rare-earth ions for rapid fluctuations of the hyperfine field⁷⁹

For arbitrary orientation of the external magnetic field relative to the crystal axes, the effective field at a rare-earth ion nucleus, as a result of thermal fluctuations of the electronic states, changes both in magnitude and direction. Because of this, the possibility of applying an adiabatic theory is excluded; however, as a consequence of the smallness of the correlation time of the random process mentioned above, it is possible to use the nonadiabatic theory of Redfield and Bloch-Wangsness⁵⁸ to analyze the behavior of the nuclear magnetization. The situation which we have chosen to study is reminiscent of the "scalar relaxation of the second kind" in liquids; however, the special behavior of the electronic angular momentum \mathbf{J} of the rare-earth ion in the crystal field and external magnetic field requires that we make some modifications in the theory in order to adapt it to anisotropic systems.

Let us write down the Hamiltonian for a spin $I = 1/2$ nucleus:

$$\mathcal{H} = -\gamma_I \hbar \mathbf{H} \mathbf{I} + A_J \mathbf{I} \mathbf{J}(t), \quad (3.13)$$

where the electron angular momentum $\mathbf{J}(t)$ depends in a random fashion on time. Let us further cast (3.13) in the form

$$\mathcal{H} = \mathcal{H}_I + \mathcal{H}'(t), \\ \mathcal{H}_I = -\gamma_I \hbar \mathbf{I} \mathbf{H}', \quad \mathbf{H}' = \mathbf{H} - \frac{A_J}{\gamma_I \hbar} \mathbf{J}_0 = (1 + \tilde{\alpha}^T) \mathbf{H}, \\ \tilde{\alpha}^T = \frac{A_J}{g_J \mu_B \gamma_I \hbar} \tilde{\chi}^T, \quad \mathcal{H}'(t) = A_J \mathbf{I} \mathbf{F}(t), \quad \mathbf{F}(t) = \mathbf{J}(t) - \mathbf{J}_0,$$

where the index 0 signifies an average using the equilibrium electronic density matrix ρ_J determined by the Hamiltonian (see 1.1):

$$\mathcal{H}_{el} = \mathcal{H}_0 + g_J \mu_B \mathbf{H} \mathbf{J}. \quad (3.14)$$

Then the ensemble average of $\mathcal{H}'(t)$ reduces to zero, while the effective nuclear Hamiltonian \mathcal{H}_1 becomes a function of temperature. For low temperatures this Hamiltonian leads to (1.6).

The equation of motion for the nuclear spin takes the form⁵⁸

$$\frac{d\langle I_\alpha \rangle}{dt} = \gamma_I \langle \mathbf{I} | \mathbf{H}' | \alpha \rangle - \sum_{\beta\beta'} j_{-\beta\beta'}(\beta\omega_0) \text{Tr} \{ (\sigma - \sigma_0) \langle [I_\alpha, I_{-\beta}] I_{\beta'} \rangle \}, \quad (3.15)$$

where $\langle \mathbf{I} \rangle = \text{Tr}(\sigma \mathbf{I})$, σ is the density matrix of the nuclear system, σ_0 is its equilibrium value, and the indices α, β distinguish the cyclic components of the vectors; the z-axis is directed along the effective field \mathbf{H}' , and ω_0 is the resonance frequency. We denote by $j_{\beta\beta'}$ the spectral density of the correlation function $K_{\beta\beta'}$ for the fluctuations of the random process:

$$j_{\beta\beta'}(\omega) = \left(\frac{A_J}{\hbar} \right)^2 \int_0^\infty K_{\beta\beta'}(t) \exp(i\omega t) dt, \quad (3.16)$$

which, as usual, is taken to be real (the imaginary part leads to an additional small level shift). As long as the hyperfine field in the excited electronic states is far larger than in the ground state ($\omega_0 \ll \Delta\omega$), and $\Delta\omega\tau_c \ll 1$, the condition $\omega_0\tau_c \ll 1$ certainly holds; this condition takes the place of the "strong narrowing" condition for which $j(\omega_0) \approx j(0)$. The $\beta \neq \beta'$ components of the tensor $j_{\beta\beta'}$ are in our case small, because Eq. (3.15) takes the form of the Bloch equations with relaxation parameters

$$\frac{1}{T_1} = j_{xx} + j_{yy}, \quad \frac{1}{T_2} = \frac{1}{2T_1} + j_{zz}. \quad (3.17)$$

Clearly, estimates of the line broadening and spin-lattice relaxation times lead to evaluation of the correlation functions $K_{\beta\beta'}(t)$.

The simplest and most transparent calculation of these quantities is a semiclassical one,⁷⁷ which reveals to us once more that the shortest lifetime of a stationary electronic state plays the role of a correlation time. However, in small magnetic fields (where the degree of smallness varies for each orientation) the splitting $\hbar\Omega$ of the excited electronic doublet can be smaller than the linewidth connected with the finiteness of the lifetime ($\sim \tau_c$). In this case, the excited states can be superpositions of the stationary doublet states, and it

becomes appropriate to calculate a quantum correlation function.

$$K_{\beta\beta'}(t) = \text{Tr} \{ \rho_J \hat{F}_{\beta'} e^{i\mathcal{H}_{el}t/\hbar} \hat{F}_\beta e^{-i\mathcal{H}_{el}t/\hbar} \}. \quad (3.18)$$

For a consistent calculation of this function, we would have to include in the Hamiltonian \mathcal{H}_{el} both the lattice and the electron-lattice interaction, which would ensure a quasi-continuum of levels associated with the lattice "heat bath"; as a result, the correlation function would be attenuated with time. In place of this approach, we will, as before, use for \mathcal{H}_{el} the Hamiltonian of an individual ion (3.14) and we will deal with the damping semi-phenomenologically, taking advantage of the presence of a characteristic time τ_c , by simply inserting into the right-hand side of (3.18) the factor $\exp(-t/\tau_c)$. Naturally, in the case of large splitting ($\Omega\tau_c \gg 1$), the correlation calculated this way coincides with the classical one.

Again, as a concrete example, we investigate the ion $^{169}\text{Tm}^{3+}$ in TmES; as before, we will consider the three lowest-lying electronic states. It is convenient to calculate the correlation function (3.18) in a basis in which the electronic Hamiltonian \mathcal{H}_{el} is diagonal. The doublet $|d_{1,2}\rangle$ in first order is split only by the parallel component of \mathbf{H} . For a given nuclear resonance frequency $\nu = \gamma_I |\mathbf{H}'|/2\pi$, the magnitude of the magnetic field, and with it the Zeeman splitting of the doublet, depend strongly on the field orientation:

$$\hbar\Omega(\theta) = 4\pi g_J \mu_B \nu \sqrt{\left(\frac{a \cos \theta'}{\gamma_{\parallel}} \right)^2 + \left(\frac{bv \sin^2 \theta'}{\gamma_{\perp}} \right)^2} \quad (3.19)$$

Here, $\gamma_{\parallel}, \gamma_{\perp}$ are the measured parameters for the nuclear spin Hamiltonian, the angle θ' determines the orientation of the field \mathbf{H}' (see Sec. 1), and

$$a = \langle d | J_z | d \rangle, \quad b = \frac{4\pi g_J \mu_B \langle 0 | J_x | d \rangle^2}{\gamma_{\perp} \Delta}. \quad (3.20)$$

The degree of mixing of $|d_1\rangle$ and $|d_2\rangle$ within the states ψ_1, ψ_2 [see (2.17)], which correspond to the Zeeman sublevels of the doublet, is also strongly dependent on the orientation of the external field:

$$\frac{q_1}{p_1} = \frac{bv \sin^2 \theta' / \gamma_{\perp}}{\sqrt{(a \cos \theta' / \gamma_{\parallel})^2 + (bv \sin^2 \theta' / \gamma_{\perp})^2} + (a \cos \theta' / \gamma_{\parallel})} \quad (3.21)$$

(the coefficients p_2, q_2 are found from the orthogonality conditions applied to ψ_1, ψ_2). Calculations lead to comparatively simple expressions for the relaxation rates, which are suitable for arbitrary magnetic field orientations:

$$T_1^{-1} = 2 \left(\frac{A_J}{\hbar} \right)^2 \tau_c \sin^2 \theta' \left[a^2 + b^2 \nu^2 \left(9 \cos^2 \theta' + \frac{1 + \cos^2 \theta'}{1 + \Omega^2 \tau_c^2} \right) \right] \exp \left(-\frac{\Delta}{kT} \right), \quad (3.22)$$

$$T_2^{-1} = (2T_1)^{-1} + 2 \left(\frac{A_J}{\hbar} \right)^2 \tau_c \left[a^2 \cos^2 \theta' + b^2 \nu^2 \sin^4 \theta' \left(9 + \frac{1}{1 + \Omega^2 \tau_c^2} \right) \right] \exp \left(-\frac{\Delta}{kT} \right). \quad (3.23)$$

Let us enumerate the basic features of the relaxation characteristics we have obtained. First of all, the relaxation rates T_1^{-1} and T_2^{-1} , in contrast to the results obtained in earlier works,^{67,89} explicitly include the hyperfine interaction constant. This result is related in an obvious way to our

use of the short correlation time condition ($A_J \tau_c \ll \hbar$), and reflects the fact that with a weakening of the hyperfine coupling the electronic motion has less influence on the nuclear relaxation. For such large correlation times it is natural to replace the factor of τ_c in expressions (3.22), (3.23) by

$\tau_c^{-1} (A_J/\hbar)^{-2} \times \langle d | J_z | d \rangle^{-2}$. The necessity for such a substitution follows from formula (3.11) for the linewidth when the field is in parallel orientation, which is valid for arbitrary fluctuation rates. As a result, relaxation parameters are obtained which are indeed independent of the hyperfine interaction. If in these expressions we consider τ_c to be due entirely to the electron-phonon interaction, then the quantity $\tau_c^{-1} \exp(-\Delta/kT)$, which now determines the relaxation time coincides with the probability of an electron spin-lattice transition from the singlet to the doublet level, which was regarded earlier as a standard measure of the nuclear relaxation rate.

Secondly, formula (3.22) predicts strongly anisotropic spin-lattice relaxation around the parallel orientation (the factor $\sin^2 \theta'$). For parallel orientation we are dealing with adiabatic conditions, and this fact is in no way connected with the size of the correlation time τ_c . For this reason, the above-mentioned anisotropy has also been deduced in previous calculations.⁸⁹ Thirdly, the line width T_2^{-1} (we remind the reader that this is the part of the width caused by the fluctuation mechanism) in parallel orientation does not depend on the resonance frequency; for other orientations this dependence has a rather complicated character, but in strong fields (which nevertheless do not violate the condition $\Omega\tau_c \lesssim 1$) it simplifies: $T_2^{-1} = c' + c''\nu^2$; c' and c'' are parameters which depend on θ and T . As distinct from T_1^{-1} , the dependence of T_2^{-1} , on orientation is rather smooth over the entire range of variation of θ .

Let us now turn to the experimental data of Refs. 64, 78, 79. Measurements of the magnitudes of α_1 for temperatures from 4.2°K to 15°K showed that the NMR line shift is strictly proportional to the paramagnetic susceptibility of the crystal (Fig. 5). This again confirms the assumption of a short correlation time. Samples of the temperature dependence of the transverse relaxation rate, obtained at various frequencies, are shown in Fig. 12. For any orientation of the

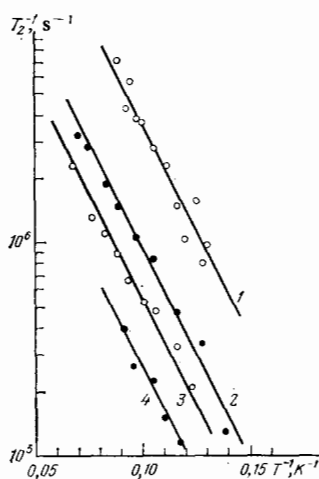


FIG. 12. Transverse relaxation rate for magnetization of ^{169}Tm nuclei in TmES as a function of reciprocal temperature.^{78,79} The external magnetic field is perpendicular to the crystal c axis; $T_2^{-1} = A \exp(-46/T)$. The resonance frequencies (lines 1 to 4) are 152, 42, 18 and 5 MHz, corresponding to pre-exponential factors of 3.53, 0.92, 0.53 and 0.25 (in units of 10^8 sec^{-1}).

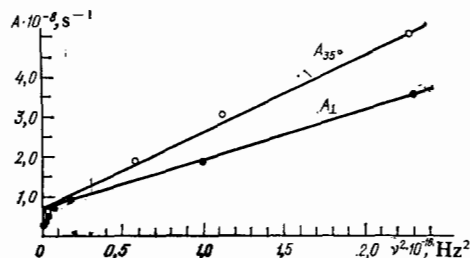


FIG. 13. Pre-exponential factor for the transverse relaxation rate of ^{169}Tm nuclei in TmES as a function of the squared resonance frequency.^{78,79} The straight lines correspond to the formulae $A_{35^\circ} = 0.6 \times 10^8 + 2.1 \times 10^{-8} \nu^2$ and $A_1 = 0.6 \times 10^8 + 1.3 \times 10^{-8} \nu^2$.

crystal in the magnetic field the relaxation rate changes with temperature according to the exponential law $T_2^{-1} = A_\theta \exp(-\Delta/kT)$ with a single parameter $\Delta = 32 \text{ cm}^{-1}$, in full correspondence with (3.23). A frequency dependence of T_2^{-1} for parallel orientation, as is expected, is not observed. For two other orientations of the crystal in the magnetic field ($\theta = 35^\circ$ and 90°) we were successful in performing measurements over a broad range of frequencies; the experimental results are shown in Fig. 13. For low frequencies, when the temperature broadening is relatively small and the line shape strongly non-Lorentzian, the precision of measurement of T_2^{-1} is insufficiently high. Such measurements at high frequencies ($\nu > 20 \text{ MHz}$) give the expected quadratic dependence: $A_\theta \sim c' + c''\nu^2$.

The results presented here convincingly argue in favor of the assumptions of our theoretical model and open up the possibility of deriving from experiment the value of the correlation time—the single adjustable parameter in Redfield's theory. And here we encounter a feature which at first glance is somewhat unexpected: the correlation times obtained in this way depend on the orientation of the external magnetic field. One of the consequences of this dependence is the noticeably large angle which the line $A_{35^\circ}(\nu^2)$ makes with the abscissa in comparison with $A_1(\nu^2)$ (Fig. 13), whereas for τ_c , which does not depend on orientation, the difference in the slopes of A_θ , according to formula (3.23), should be very small. The dependence of τ_c on θ is very evident in the experiments which measure T_1 . The orientational dependence of $T_1^{-1}(\theta)$ for $T = 4.25^\circ\text{K}$ is displayed in Fig. 14. A sharp decrease in T_1^{-1} as $\theta \rightarrow 0$ predicted by the theory is clearly

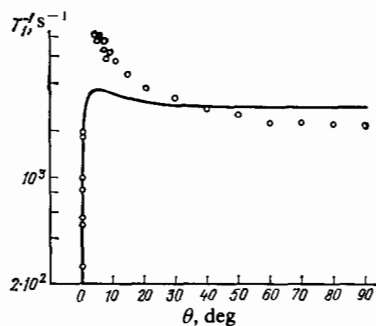


FIG. 14. Orientation dependence of the spin-lattice relaxation rate for ^{169}Tm nuclei in TmES at a temperature of 4.2°K. The resonance frequencies are 7.5 MHz for $\theta = 0$ to $\theta = 50^\circ$, and 13 MHz for $\theta = 3^\circ$ to $\theta = 90^\circ$. The solid line is calculated using formulas (2.22) and (3.22).

manifested; however, by virtue of the extremely strong anisotropy of the tensor $\tilde{\alpha}$, the magnitude of $\sin^2 \theta'$ is close to unity in the angular interval $3^\circ \leq \theta < 90^\circ$; thus the observed growth (roughly by a factor of four) in the nuclear spin-lattice relaxation rate for a change in θ from 90° to 7.5° can only be due to the growth of the correlation time τ_c .

If the lifetime of an ion in an excited state were regulated by the ground-state electron-vibronic interaction, then τ_c^{-1} would be the probability of a spontaneous transition of an ion into the ground state with emission of a phonon of energy $\Delta \pm \hbar \Omega/2$. As long as $\hbar \Omega$ is much smaller than Δ for all orientations, any dependence of τ_c^{-1} on θ due to variation of $\hbar \Omega$ must be completely negligible. In this way, we are led to the conclusion that the lifetime of the Tm^{3+} ion in an excited state is determined for the most part by interparticle interactions of dipole-dipole type, quadrupole-quadrupole type, or through the phonon field. Approximate estimates of $\tau_c(\theta)$, developed in subsection 2d are in qualitative, and to a significant degree quantitative, agreement with experiment (Fig. 14).

In the perfectly parallel orientation $\mathbf{H} \parallel c$, a small transverse component of the hyperfine field which induces relaxation transitions can be present as a consequence of local distortions of the symmetry of the crystal potential. The local distortions can be both static (structural defects) and dynamic, i.e., caused by lattice vibrations. In insufficiently perfect crystals this effect can almost entirely mask the sharp dip in T_1^{-1} in the vicinity of $\theta = 0$, which apparently is what is occurring in LiTmF_4 (Refs. 67, 76).

e) Relaxation of nuclei of diamagnetic atoms

As a result of electrons from the ground-state shell of the rare-earth ions making transitions between various states, the magnetic field varies randomly not only at the nuclei of the RE ions themselves, but also at the nuclei of paramagnetic impurity centers and neighboring diamagnetic atoms, such as at ^{19}F atoms in LiTmF_4 or protons of TmES . Such fluctuations can in turn induce relaxation at these magnetic centers also. For the case of nuclear resonance of ^{19}F and ^1H , the condition for rapid fluctuations $\omega_0 \tau_c \ll 1$ is fulfilled with a wide margin, and for calculating the spin-lattice relaxation time one can use formulae (3.16)–(3.18). Thus, the interaction between the above-mentioned nuclei and the $4f$ rare-earth ions' electrons can be regarded as a random process. Of the possible interactions, the most obvious is the magnetic dipole-dipole interaction; the perturbation Hamiltonian in this case can be written in the form

$$\mathcal{H}'(t) = \gamma_i \hbar g_J \mu_B \sum_{i\beta\beta'} B_{\beta\beta'}^{(i)} I_\beta (J_\beta^{(i)} - J_{0\beta}^{(i)}), \quad (3.24)$$

$$B_{\beta\beta'}^{(i)} = r_i^{-3} \left(\delta_{\beta\beta'} - \frac{3r_{i\beta} r_{i\beta'}}{r_i^2} \right).$$

Here the summation is over the rare-earth ions surrounding the nucleus, while r_i is the distance from the nucleus to the i th ion. Let us rewrite (3.24) in the form

$$\mathcal{H}'(t) = \gamma_i \hbar g_J \mu_B \mathbf{I} \mathbf{G}(t),$$

where

$$\mathbf{G}_\beta(t) = \sum_{i\beta'} B_{\beta\beta'}^{(i)} (J_\beta^{(i)}(t) - J_{0\beta}^{(i)}).$$

We will consider the fluctuations of different ions to be uncorrelated; this approximation is correct when each ion has a large number of neighbors. Then the correlation function for the random quantity $\mathbf{G}(t)$ is easily expressed in terms of the single-ion correlation function $K_{\beta\beta'}(t)$ which was already introduced in the previous section

$$K'_{\beta\beta'}(t) = \langle G_\beta(t) G_{\beta'} \rangle = \sum_{i\beta''\beta'''} B_{\beta\beta''}^{(i)} B_{\beta''\beta'''}^{(i)} \langle F_{\beta''}(t) F_{\beta'''} \rangle.$$

Here, the angular brackets denote an average with respect to the equilibrium distribution function (classical or quantum). Correspondingly, the relaxation times also can be expressed in terms of the spectral functions of the previous subsection and a few lattice sums, for example

$$T_1^{-1} = \left(\frac{\gamma_i \hbar g_J \mu_B}{A_T} \right)^2 \sum_{i\beta\beta'} (B_{X\beta}^{(i)} B_{X\beta'}^{(i)} + B_{Y\beta}^{(i)} B_{Y\beta'}^{(i)}) j_{\beta\beta'}(0). \quad (3.25)$$

We remind the reader that the Z -axis is here directed along the effective magnetic field \mathbf{H}_{eff} at the diamagnetic atom, and that the difference in direction between \mathbf{H}_{eff} and \mathbf{H} is not as marked as for the nuclei of the basic rare-earth ions. For a three-level system of the type discussed earlier we can write out the relaxation times for the case $\mathbf{H} \parallel c$ (in this case the only component of the spectral density different from zero is j_{cc}):

$$\begin{aligned} T_1^{-1} &= 18 \gamma_i^2 g_J^2 \mu_B^2 \tau_c \langle d | J_z | d \rangle^2 \sum_i r_i^{-6} \sin^2 \theta_i \cos^2 \theta_i \exp\left(-\frac{\Delta}{kT}\right), \\ T_2^{-1} &= \gamma_i^2 g_J^2 \mu_B^2 \tau_c \langle d | J_z | d \rangle^2 \sum_i r_i^{-6} [9 \sin^2 \theta_i \cos^2 \theta_i \\ &\quad + 2(1 - 3 \cos^2 \theta_i)^2] \exp\left(-\frac{\Delta}{kT}\right). \end{aligned} \quad (3.26)$$

Here, θ_i is the angle between the c -axis and the radius vector r_i . In Fig. 15 we show the results of measurements of T_1 for the ^{19}F nuclei in LiTmF_4 .⁷⁶ The dashed line gives a calculated result: $T_1^{-1} = 1.25 \cdot 10^3 \exp(-46/T)$ from formula

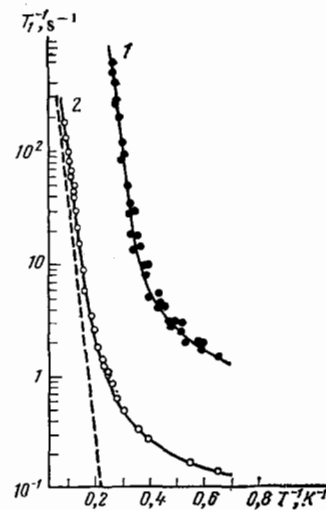


FIG. 15. Spin-lattice relaxation of nuclei of ^{169}Tm (curve 1) and ^{19}F (curve 2) in LiTmF_4 with an impurity concentration of 0.01% Er^{3+} .⁷⁶ The external field was parallel to the c -axis, the resonance frequency was 10.6 MHz. The dashed line is the calculated relaxation rate for ^{19}F [see (3.26), (2.18)].

(3.26), using the necessary data on crystal structure,⁹⁰ the wave function of the Tm^{3+} ion in the crystal field,^{26,57} and also the value $\tau_c = 1.2 \times 10^{-11}$ sec, which is obtained from formula (2.18) for the probability of a dipole-dipole transition of the excitation to a neighboring ion. Agreement with experiment should be acknowledged as being entirely satisfactory, keeping in mind that the calculation was performed without using any adjustable parameters.

We note also that if NMR of the nuclei of the diamagnetic atoms is sampled often and up to significantly higher temperatures than for nuclei of the basic rare-earth ions, the low temperature condition $W_0 \gg W_1$, W_2 ceases to hold, and this leads to complicated expressions for the correlation functions. Thus, in (3.26) for $W_1 \approx W_2$, in place of the factor $\exp(-\Delta/kT)$ we will have $[1 + 4 \exp(-2\Delta/kT)] \times [1 + 2 \exp(-\Delta/kT)]^{-3} \exp(-\Delta/kT)$. With an increase in temperature other complications emerge which are difficult to take into account quantitatively, e.g., the populating of higher-lying levels and the appearance of a temperature dependence of the correlation time τ_c . For example, for $kT \gg \Delta$, the electron-phonon contribution to τ_c^{-1} depends linearly on temperature, because at high temperatures stimulated transitions to the ground state predominate over the spontaneous ones.

Paramagnetic impurity centers with small intrinsic relaxation rates to the lattice of the type associated with S -state ions can be even more effective in relaxing neighboring rare-earth ions by means of fluctuations. In this case, the small-correlation-time condition, in view of the large EPR frequency, will obviously often be violated. Under these circumstances, the relaxation times can be calculated approximately from formulae (3.25) and (3.26), substituting ($\gamma_I \hbar/\mu_B$) for the g -factor of the impurity ion.

d) Relaxation via paramagnetic impurities

The effectiveness of relaxation processes which are connected with thermal excitation of electronic states of the basic RE ions decreases as the temperature falls according to $\exp(-\Delta/kT)$. For sufficiently low temperatures, the usual nuclear relaxation mechanism for dielectrics via paramagnetic impurity centers comes into play. This is clearly in evidence in Fig. 15: the temperature variations of the relaxation rates of the ^{19}F nuclei for $T < 5$ °K and the ^{169}Tm nuclei for $T < 3$ °K slow down abruptly, and for very low temperatures the nuclear moments of thulium relax at most ten times faster than the fluorine nuclei. The latter fact shows clearly that relaxation of unlike nuclei proceeds by a single channel, namely by paramagnetic impurities. The observed factor-of-ten difference in the rates T_1^{-1} is easily obtained, once one multiplies the concentration ratio ($n_{Tm}/n_F = 1/4$) by the square of the ratio of their magnetic moments ($\gamma_{Tm}^2/\gamma_F^2 = 36$). The character of the relaxation processes which take place in such complex systems, which consist of a nuclear Zeeman reservoir (I) with heat capacity c_I , a dipole-dipole reservoir (DDR) of impurities (d) with heat capacity c_d , and a lattice-vibration reservoir (l), depends on the relation between the rates at which thermal equilibrium is established between its constituent parts.

Let us examine the conditions for relaxation of the thulium nuclei in axially-symmetric crystals of the $LiTmF_4$ and $TmES$ type, confining ourselves to the case of a magnetic field oriented along the c -axis. For estimates of the relaxation rates, we will use well-known relations,^{59,91-93} modifying them to correspond to the problem at hand. Thus, we set the spin-spin relaxation rate of paramagnetic centers τ_2^{-1} equal to the Larmor frequency of a spin S in the local field created by the neighboring impurity spins:

$$\tau_2^{-1} = \frac{g_{\perp}^2 \mu_B^2 f_6}{\hbar a^3}$$

(a is the crystal lattice constant). We note that in this formula we have used the value g_{\perp} , since the rate τ_2^{-1} is determined by the oscillating local field created by the transverse components of the magnetic moment of the impurity ion. It is reasonable to use the second moment of the impurity EPR line [see (2.11)] as a "mean-square NMR frequency":

$$\omega_d^2 = \frac{(2g_{\parallel}^2 + g_{\perp}^2) \mu_B^2 f_6^2 \Sigma_6}{16\hbar^2}$$

Nuclear relaxation via paramagnetic impurities is caused by interactions of the type $I-S_z$, i.e., interactions between the transverse components of the nuclear moment and longitudinal components of the electronic moment. Thus, in order to investigate the relaxation of thulium nuclei in a magnetic field $H \parallel c$, we must use the quantities γ_{\perp} and g_{\parallel} in the well-known formulae for the rate of energy transfer from the nuclear Zeeman reservoir to the lattice (T_{Il}^{-1}) and DDR impurities (T_{Id}^{-1}). As a result, all the information of interest to us on the relaxation of nuclei of Van Vleck ions via impurity centers is lumped into the following relations:

$$\begin{aligned} T_{Il}^{-1} &\approx \frac{2\pi}{5} \frac{\gamma_{\perp}^2 g_{\parallel}^2 \mu_B^2 f_6^2 n_{Tm}}{d^3 \omega_d^2 \tau_1} \operatorname{sch}^2 \frac{g_{\parallel} \mu_B H}{2kT}, \\ T_{Id}^{-1} &\approx \frac{2\pi}{5} \frac{\gamma_{\perp}^2 g_{\parallel}^2 g_{\perp}^2 \mu_B^4 f_6^2 n_{Tm}}{\hbar d^3 \omega_d^2} \operatorname{sch}^2 \frac{g_{\parallel} \mu_B H}{2kT}, \\ T_{dI}^{-1} &= \frac{c_I}{c_d} T_{Id}^{-1}, \quad T_{dI}^{-1} = (2-5) \tau_1^{-1}, \\ \frac{c_I}{c_d} &= \frac{16\hbar^2 \omega_d^2}{f_6 (2g_{\parallel}^2 + g_{\perp}^2) \mu_B^4 \Sigma_6}. \end{aligned} \quad (3.27)$$

Here, d is the radius of the spin diffusion barrier, n_{Tm} is the concentration of Van Vleck ions, T_{dI}^{-1} and T_{Id}^{-1} are the rates of energy transfer from the DDR impurities to the nuclear Zeeman and lattice reservoirs, respectively; τ_1 is the impurity spin-lattice relaxation time.

Let us now turn to experiment.⁶⁷ In Fig. 16 we show results of measurements of the relaxation rates of the longitudinal magnetization of thulium nuclei in three crystals of $LiTmF_4$, containing the impurity ion Er^{3+} in the following concentrations: $f_{Er} = 1 \times 10^{-4}$ (1), 4×10^{-4} (2), and 3×10^{-3} (3). As is clear, for the lowest temperatures the relaxation rate does not depend on temperature, while its functional dependence on impurity concentration is close to quadratic. Let us undertake to calculate an estimate of the rate T_{Id}^{-1} . Taking into account that the Er^{3+} ion possesses a large magnetic moment ($g_{\parallel} = 2.960$, $g_{\perp} = 8.074$)⁷⁶ we get a radius for the diffusion barrier equal to 20 Å. Then for the three samples of $LiTmF_4$ that have been studied, the following values of T_{Id}^{-1} are obtained: sample 1—2.6 sec⁻¹, sample 2—41 sec⁻¹, sample 3— 2.3×10^3 sec⁻¹. The corresponding

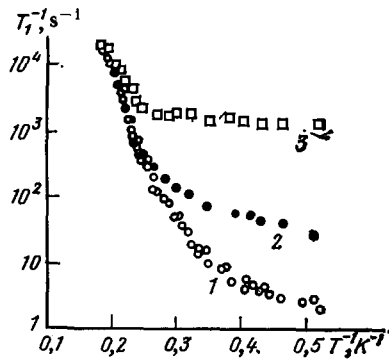


FIG. 16. Spin-lattice relaxation of ^{169}Tm nuclei in LiTmF_4 with an impurity concentration of 0.01% (curve 1), 0.04% (curve 2) and 0.3% (curve 3) of Er^{3+} ions.⁶⁷ The external magnetic field was parallel to the c axis of the crystal, the resonance frequency was 10.6 MHz.

experimental values of the longitudinal relaxation rates T_1^{-1} —for sample 1, 2 sec^{-1} , sample 2, 30 sec^{-1} , and sample 3, $1.3 \times 10^3 \text{ sec}^{-1}$ —confirm that the quantity d was reasonably chosen. Detailed estimates of the rates (3.27), using well-known values⁷⁶ for the time τ_1 show that in the example under discussion, the inequalities $T_{\text{td}}^{-1}, T_{\text{dt}}^{-1} \ll T_{\text{dl}}^{-1}$ are realized, and the relaxation rate for longitudinal magnetization of the thulium nuclei measured in a high magnetic field coincides with the energy transfer rate from the nuclear Zeeman reservoir to the DDR (Er^{3+}) impurity centers. Thus, for low temperatures the spin-lattice relaxation of nuclei of Van Vleck ions in crystals which contain paramagnetic impurities does not differ in principle from nuclear relaxation of diamagnetic atoms. Here, the role of the 4f electrons is only to enhance the dipole-dipole interactions of the nuclei with paramagnetic centers on account of which the rate of nuclear relaxation appears larger than usual by a factor of $(1 + \alpha)^2$.

We note that for very low temperatures ($kT \ll g_{\parallel} \mu_B H$), where there is significant electronic polarization due to the impurity ions, the effectiveness of the relaxation mechanism discussed here will, according to (3.27), once again decrease sharply. It is precisely this phenomenon which gives rise to the well-known “freezeout” effect of the nuclear polarization.⁹⁴ In this case, evidently, the nuclear spin-lattice relaxation comes about via direct energy transfer from the spins to the lattice.

e) One-phonon relaxation processes and nuclear acoustic resonance

In addition to real transitions between electronic states, caused, let us say, by dipole-dipole or electron-vibronic ion interactions, there are other effects which can modulate the hyperfine field at the rare-earth ion nuclei. Lattice vibrations perturb the crystal potential, and thus can lead to a small variation in the magnetization in each of the electron states, including the ground-state singlet state. Because of this variation, there arises the possibility of direct relaxation transitions between nuclear sublevels with emission or absorption of a single phonon of the appropriate frequency. The effective spin-phonon interaction Hamiltonian has the following form

$$\mathcal{H}'_{\text{eff}} = G_{\alpha\beta\gamma\delta} (I_{\alpha} H_{\beta} + I_{\beta} H_{\alpha}) e_{\gamma\delta} + P_{\alpha\beta\gamma\delta} I_{\alpha} I_{\beta} e_{\gamma\delta} \equiv U_{\gamma\delta} e_{\gamma\delta}, \quad (3.28)$$

where $e_{\gamma\delta}$ is the deformation tensor. If the nuclear spin $I = 1/2$, then only the first term is present in $\mathcal{H}'_{\text{eff}}$. The spin-phonon interaction constant can be expressed in terms of the deformation potential:

$$\Delta V = \sum_{\alpha\beta} V_{\alpha\beta} e_{\alpha\beta}, \quad (3.29)$$

if in the formula determining the effective nuclear spin Hamiltonian in the ground state we write the electron wave function and energy intervals to first order in the perturbation Δv . As a result we obtain

$$G_{\alpha\beta\gamma\delta} = g_J \mu_B A_J (\langle 0 | J_{\alpha} C_0 V_{\gamma\delta} C_0 J_{\beta} + J_{\alpha} C_0 J_{\beta} C_0 V_{\gamma\delta} + V_{\gamma\delta} C_0 J_{\alpha} C_0 J_{\beta} | 0 \rangle - \langle 0 | V_{\gamma\delta} | 0 \rangle \langle 0 | J_{\alpha} C_0 J_{\beta} | 0 \rangle), \quad (3.30)$$

where the energy and wave functions are of zero order with respect to the deformation perturbation. The form of the tensor $P_{\alpha\beta\gamma\delta}$ is precisely the same, only in place of the coefficient $g_J \mu_B$ in (3.30) the hyperfine interaction constant A_J should appear. The electron-phonon interaction constants in (3.29) can in principle be calculated on the basis of refinements of crystal field theory,⁹⁵ or found from experiments on the change in spin-lattice relaxation of paramagnetic impurity ions with pressure. We note that for magnetic fields usually used in experiments, i.e., of magnitude of a few kilosterds, the contribution to the relaxation of nuclear spins with $I > 1/2$ from the first term of $\mathcal{H}'_{\text{eff}}$ (3.28) is comparable in magnitude and even exceeds somewhat the contribution of the second terms, whereas for electron spins, as a rule, the most important contribution to the relaxation comes from components of the Hamiltonian which are quadratic in the spin variables.⁸⁷

If the Debye model is used to describe the lattice vibrations, the relaxation rate for transitions between nuclear sublevels i, f can be written in standard form⁹⁶:

$$T_1^{-1} = w_{if} + w_{fi} = \frac{\omega_0^2}{6\pi\hbar d_0 v^5} \text{cth} \left(\frac{\hbar\omega_0}{2kT} \right) \sum_r q_r |\langle i | U_r | f \rangle|^2, \quad (3.31)$$

where ω_0 is the transition frequency, d_0 the crystal density, $1/v^5 = (2/5v_l^5) + (3/5v_t^5)$, and v_l and v_t are the longitudinal and transverse sound velocities; U_r is a combination of components of the second-rank tensor $U_{\gamma\delta}$ determined by Eq. (3.28) which transforms under rotations like a set of normalized real-valued spherical harmonics. The coefficients g_r in (3.31) are quantities of order unity.

Abragam and Bleaney¹⁶ suggested the following approach for making approximate estimates of the relaxation times (3.31). We confine ourselves to investigating only those terms in $\mathcal{H}'_{\text{eff}}$ which are linear in the field. Then in the matrix element of the operator U_r , we can separate out the factor $g_J \mu_B A_J H |J|/\Delta$, where $|J|$ is a quantity of the same order of magnitude as the matrix elements of the operator J_{α} . In absolute value, this factor is of just the same order of magnitude as the energy $\hbar\omega_0$, whereas the remaining part of the matrix element $\langle i | U_r | f \rangle$ can be approximately represented by the form $\langle 0 | V_r C_0 J | 0 \rangle$. But just this expression is

obtained when we calculate the relaxation rate for transitions between states i, f of the electronic Kramers doublet mediated by the interactions (3.29), since the matrix elements $\langle i | V_r | f \rangle$ are different from zero only because of the first-order correction to the states i, f due to the magnetic field. The only difference between the nuclear and electronic situations involve the resonance frequencies; this difference is evident in the expression:

$$T_{1\text{nuc}}^{-1} \approx \tau_{1\text{el}}^{-1} \left(\frac{\omega_{\text{nuc}}}{\omega_{\text{el}}} \right)^5 \text{cth} \left(\frac{\hbar\omega_{\text{nuc}}}{2kT} \right) \text{th} \frac{\hbar\omega_{\text{el}}}{2kT}, \quad (3.32)$$

where $\tau_{1\text{el}}$ is the electronic spin-lattice relaxation time of Kramers rare-earth ions with splittings comparable to Δ in the crystal field, and which are embedded in a host matrix with the appropriate density and sound velocity.

The relaxation mechanism we are discussing here is very weak. According to Vařfel'd's calculation,⁸⁹ the relaxation time for ¹⁶⁹Tm nuclei in TmEs for a temperature of 4.2 °K in a field of 500 oersteds perpendicular to the c -axis of the crystal must be of the order of 10^{11} sec. However, the probability of a direct relaxation transition grows with increasing magnetic field as H^4 . Assuming $H = 80$ kilo-oersteds, we obtain $T_1 = 150$ sec at $T = 0.02$ °K. Clearly, these estimates hold out some hope that by using the spin system of Van Vleck ion nuclei one may be successful in cooling to ultralow temperatures by "brute force" methods.

The method of nuclear acoustic resonance proves to be suitable for studying the nuclear spin-phonon interaction using a moderate magnetic field. Resonance absorption of ultrasound can be regarded as the inverse phenomenon to magnetic relaxation,⁸⁷ since it too is mediated by one-phonon processes. Therefore, the considerations discussed earlier are relevant also to the making of estimates of the magnitude of absorption of sound by nuclei of Van Vleck ions. The absorption coefficient of sound⁸⁷ due to transitions between nuclear sublevels i, f takes the form

$$\alpha_{if}^{\text{ac}} = \frac{\pi n \omega_0}{\hbar d_0 v^3} g(\omega) \text{th} \left(\frac{\hbar\omega_0}{2kT} \right) \left| \sum_{\mathbf{r}} \langle i | U_r | f \rangle e_r \right|^2, \quad (3.33)$$

where n is the nuclear concentration, $g(\omega)$ is the form factor of the NMR line normalized to unity, e_r is analogous to U_r , i.e., a spherical-tensor combination of the components of the rank-two tensor $\lambda_\alpha \varphi_\beta$ consisting of a unit vector in the direction of propagation of sound λ and its polarization φ . Due to the high concentration of absorbing centers and the frequency, which is large compared to what is usual in NMR, one obtains the magnitudes of the above-mentioned coefficients wholly from experimental measurements. The first nuclear acoustic resonance observed in a Van Vleck paramagnet was detected in praseodymium trifluoride³³; the resonant ion was ¹⁴¹Pr ($I = 5/2$). The measurement was conducted at a temperature of 4.2 °K using longitudinal ultrasound frequencies from 21 to 36 MHz. An estimate of the absorption coefficient gave a value of the quantity $\sigma \sim 10^{-6}$ cm⁻¹. Strong resonance absorption ($\sigma \sim 3$ cm⁻¹ for $T = 1.6$ °K) of longitudinal acoustic waves with frequency 800 MHz in single-crystal HoVO₄ were seen by Bleaney *et al.*⁹⁷ By studying resonance absorption of sound in various propagation directions and polarizations one can obtain almost all the spin-phonon interaction constants, and along

with them reliable estimates of the one-phonon relaxation rates of Van Vleck ion nuclei.

CONCLUSION

Summing up this discussion of nuclear magnetic resonance in rare-earth Van Vleck paramagnets, we remark that most of the observable aspects of the phenomena are successfully explained by the interaction of the nuclei with the residual electronic magnetic moments of the RE ions in the singlet ground state, and by the modulation of this interaction due to the coupling of the electronic moments among themselves and with the lattice vibrations of the crystal. For low temperatures ($kT \ll \Delta$), the pattern of the NMR spectra reduces to one which was well-understood and described some time ago.^{15,16} With an increase in temperature (beginning at liquid helium temperatures or higher) the most important of the above-mentioned phenomena turns out to be modulation of the hyperfine interaction, resulting from real transitions of the Van Vleck ions between the ground state and the nearest excited states. We have described the temperature dependence of the shift and broadening of NMR lines, the spin-lattice relaxation times for nuclei within Van Vleck ions and nuclei within diamagnetic ions, and also the frequency and orientation dependences of these quantities, within the framework of a single simple theory based on the assumption of a hyperfine interaction Hamiltonian which varies randomly with time. This theory agrees with experiment not only qualitatively, but also to a significant degree quantitatively; moreover, the agreement is obtained without resort to any adjustable parameters. We have studied the electronic excitations of Van Vleck ions by viewing them as localized quasiparticles, diffusing in a random fashion between lattice sites. This theory can be further refined by interpreting these excitations as excitons in molecular crystals.⁹⁸ It is also useful to take a more rigorous look at the case of intermediate fluctuation rates ($\omega_0 \tau_c \sim 1$), which is encountered in EPR of impurity ions.^{28,29}

At present, the focus of intense experimental investigation of nuclear magnetism in Van Vleck paramagnets, along with nuclear magnetism in general, has moved to the area of ultralow temperatures. Here, the most interest attaches to such problems as nuclear magnetic ordering,^{16,83,84,99,100} coupling of nuclear spin systems with other spins in the crystal and with the crystal lattice,^{31,32,43,44} and direct contact of the nuclear spins in the solid state with nuclei in a liquid He³ environment.^{85,101} A marked slowing down of nuclear relaxation processes makes experiments at ultralow temperatures very protracted and complicated. One can hope that the special peculiarities of Van Vleck paramagnets will significantly alleviate this situation, and thereby open up new possibilities for NMR experiments.

¹Translation editor's note: The numerator of Eq. (3.2) which is *quadratic* in the W_i appears to be inconsistent with the expression $I(\omega) = \text{Re}(W A^{-1} \mathbf{1})$ preceding it which is *linear* in the W_i .

²M. M. Zaripov, *Izv. Akad. Nauk SSSR Ser. Fiz.* **22**, 1220 (1956).

³R. J. Elliott, *Proc. Phys. Soc.* **70**, 119 (1957).

⁴S. A. Al'tshuler and V. N. Yastrebov, *Zh. Eksp. Teor. Fiz.* **47**, 382 (1964) [*Sov. Phys. JETP* **20**, 254 (1965)].

- ⁴S. A. Al'tshuler and M. A. Teplov, *Pis'ma Zh. Eksp. Teor. Fiz.* **5**, 209 (1967) [*JETP Lett.* **5**, 167 (1967)].
- ⁵S. A. Al'tshuler, *Pis'ma Zh. Eksp. Teor. Fiz.* **3**, 177 (1966) [*JETP Lett.* **3**, 112 (1966)].
- ⁶K. Andres and E. Bucher, *Phys. Rev. Lett.* **21**, 1221 (1968).
- ⁷K. Andres and E. Bucher, *J. Appl. Phys.* **42**, 1522 (1971).
- ⁸R. M. Mineeva, *Fiz. Tverd. Tela (Leningrad)* **5**, 1403 (1963) [*Sov. Phys. Solid State* **5**, 1020 (1963)].
- ⁹R. M. Mineeva, *Fiz. Tverd. Tela (Leningrad)* **8**, 2222 (1966) [*Sov. Phys. Solid State* **8**, 1764 (1967)].
- ¹⁰L. Ta. Shekun, *Fiz. Tverd. Tela (Leningrad)* **8**, 2929 (1966) [*Sov. Phys. Solid State* **8**, 2340 (1967)].
- ¹¹M. A. Teplov, *Zh. Eksp. Teor. Fiz.* **53**, 1510 (1967) [*Sov. Phys. JETP* **26**, 872 (1968)].
- ¹²M. A. Teplov, *Fiz. Tverd. Tela (Leningrad)* **10**, 2548 (1968) [*Sov. Phys. Solid State* **10**, 2009 (1969)].
- ¹³S. A. Al'tshuler, F. L. Aukhadeev, and M. A. Teplov, *Pis'ma Zh. Eksp. Teor. Fiz.* **9**, 46 (1969) [*JETP Lett.* **9**, 26 (1969)].
- ¹⁴S. L. Tsarevskii, *Fiz. Tverd. Tela (Leningrad)* **12**, 2047 (1970) [*Sov. Phys. Solid State* **12**, 1625 (1971)].
- ¹⁵S. A. Al'tshuler and M. A. Teplov, *Problemy magnitogo rezonansa (Problems in Magnetic Resonance)*, Nauka, M., 1978, p. 14. M. A. Teplov, *Proc. 2nd Int. Conf. on Crystal Field Effects in Metals and Alloys*, Zurich (Ed. A. Furrer) Plenum Press, N. Y., 1977, p. 318.
- ¹⁶A. Abragam and B. Bleaney, *Proc. R. Soc. London A* **387**, 221 (1983).
- ¹⁷E. J. Veenendaal, H. B. Brom, and W. J. Huiskamp, *Physica B* **121**, 1 (1983).
- ¹⁸L. E. Erickson, *Phys. Rev. B* **16**, 4731 (1977).
- ¹⁹R. M. Shelby and R. M. Macfarlane, *Phys. Rev. Lett.* **47**, 1172 (1981).
- ²⁰L. Nielsen, *J. Less-Common Metals* **94**, 243 (1983).
- ²¹V. Zevin and E. Barboy, *Z. Phys. B* **39**, 173 (1980).
- ²²G. A. Gering and K. A. Gering, *Rep. Prog. Phys.* **31**, 1 (1975).
- ²³K. P. Belov, G. I. Kataev, R. Z. Levitin, S. A. Nikitin, and V. I. Sokolov, *Usp. Fiz. Nauk* **140**, 271 (1983) [*Sov. Phys. Usp.* **26**, 518 (1983)].
- ²⁴S. A. Al'tshuler, V. I. Krotov, and B. Z. Malkin, *Pis'ma Zh. Eksp. Teor. Fiz.* **32**, 232 (1980) [*JETP Lett.* **32**, 215 (1980)].
- ²⁵B. Luthi, M. E. Mullen, and E. Bucher, *Phys. Rev. Lett.* **31**, 95 (1973).
- ²⁶F. L. Aukhadeev, R. Sh. Zhdanov, M. A. Teplov, and D. N. Terpilovskii, *Fiz. Tverd. Tela (Leningrad)* **23**, 2225 (1981) [*Sov. Phys. Solid State* **23**, 1303 (1981)].
- ²⁷R. T. Harley and D. I. Manning, *J. Phys. C* **11**, L633 (1978).
- ²⁸F. Mehran and K. W. H. Stevens, *Phys. Rep.* **85**, 123 (1982).
- ²⁹F. Mehran, K. W. H. Stevens, T. S. Plaskett, and W. J. Fitzpatrick, *Phys. Rev. B* **27**, 548 (1983).
- ³⁰I. S. Konov and M. A. Teplov, *Fiz. Tverd. Tela (Leningrad)* **18**, 853 (1976) [*Sov. Phys. Solid State* **18**, 490 (1976)].
- ³¹F. L. Aukhadeev, V. A. Grevtsev, I. S. Konov, M. S. Tagirov, and M. A. Teplov, *Fiz. Tverd. Tela (Leningrad)* **18**, 2107 (1976) [*Sov. Phys. Solid State* **18**, 1228 (1976)].
- ³²M. A. Teplov, M. Shtaudte, and G. Feller, *Fiz. Tverd. Tela (Leningrad)* **22**, 2460 (1980) [*Sov. Phys. Solid State* **22**, 1433 (1980)].
- ³³S. A. Al'tshuler, A. V. Duglav, A. Kh. Khasanov, I. G. Bol'shakov, and M. A. Teplov, *Pis'ma Zh. Eksp. Teor. Fiz.* **29**, 680 (1979) [*JETP Lett.* **29**, 624 (1979)].
- ³⁴I. S. Konov and M. A. Teplov, *Fiz. Tverd. Tela (Leningrad)* **19**, 285 (1977) [*Sov. Phys. Solid State* **19**, 163 (1977)].
- ³⁵B. Bleaney, F. N. H. Robinson, S. H. Smith, and M. R. Wells, *J. Phys. C* **10**, L385 (1977).
- ³⁶B. Bleaney, R. T. Harley, J. F. Ryan, M. R. Wells, and M. C. K. Wiltshire, *J. Phys. C* **11**, 3059 (1978).
- ³⁷B. Bleaney, A. G. Stephen, P. J. Walker, and M. R. Wells, *Proc. R. Soc. London A* **381**, 1 (1982).
- ³⁸B. Bleaney, F. N. H. Robinson, M. R. Wells, *Proc. R. Soc. London A* **362**, 179 (1978).
- ³⁹A. V. Egorov, L. D. Livanova, M. S. Tagirov, and M. A. Teplov, *Fiz. Tverd. Tela (Leningrad)* **22**, 2836 (1980) [*Sov. Phys. Solid State* **22**, 1655 (1980)].
- ⁴⁰E. D. Jones, *J. Phys. Chem. Solids* **29**, 1305 (1968).
- ⁴¹E. D. Jones and V. H. Schmidt, *J. Appl. Phys.* **40**, 1406 (1969).
- ⁴²B. Bleaney and M. R. Wells, *Proc. R. Soc. London A* **370**, 131 (1980).
- ⁴³H. Suzuki, T. Inoue, Y. Higashino, and T. Ohtsuka, *Phys. Lett. A* **77**, 185 (1980).
- ⁴⁴H. Suzuki, T. Inoue, and T. Ohtsuka, *Physica B* **107**, 563 (1981).
- ⁴⁵H. Suzuki, Y. Higashino, and T. Ohtsuka, *J. Low Temp. Phys.* **41**, 449 (1980).
- ⁴⁶B. Bleaney, J. H. T. Pasman, and M. R. Wells, *Proc. R. Soc. London A* **387**, 75 (1983).
- ⁴⁷B. Bleaney, J. F. Gregg, M. J. M. Leask, and M. R. Wells, *J. Magn. Magn. Mater.* **31-34**, 1061 (1983).
- ⁴⁸B. Bleaney, *Proc. R. Soc. London A* **376**, 217 (1981).
- ⁴⁹E. D. Jones, *Phys. Rev. Lett.* **19**, 432 (1967).
- ⁵⁰E. D. Jones, *Colloq. Int. C. N. R. S.* **2**, 495 (1970).
- ⁵¹H. T. Weaver and J. E. Schirber, *Phys. Rev. B* **14**, 951 (1976).
- ⁵²H. T. Weaver, J. E. Schirber, and B. Morosin, *Solid State Commun.* **23**, 785 (1977).
- ⁵³N. Kaplan, D. L. Williams, and A. Grayevsky, *Phys. Rev. B* **21**, 899 (1980).
- ⁵⁴A. A. Kosov and S. L. Tsarevskii, *Fiz. Tverd. Tela (Leningrad)* **17**, 2306 (1975) [*Sov. Phys. Solid State* **17**, 1525 (1975)].
- ⁵⁵K. Satoh, Y. Kitaoka, H. Yasuoka, S. Takayanagi, and T. Sugawara, *J. Phys. Soc. Jpn.* **50**, 351 (1981).
- ⁵⁶R. G. Barnes, R. L. Mossbauer, E. Kankeleit, and J. M. Poindexter, *Phys. Rev. A* **136**, 175 (1964).
- ⁵⁷F. L. Aukhadeev, R. Sh. Zhdanov, M. A. Teplov, and D. N. Terpilovskii, *Paramagnitnii rezonans (Paramagnetic Resonance)*, Kazan' (Publ. Univ. Kazan', 1983), no. 19, p. 3.
- ⁵⁸A. Abragam, *The Principles of Nuclear Magnetism*, Clarendon Press, Oxford, 1961 [Russ. Transl., IL, M., 1963].
- ⁵⁹V. A. Atsarkin, *Dinamicheskaya polarizatsiya yader v tverdykh dielektrikakh (Dynamic Nuclear Polarization in Solid Dielectrics)*, Nauka, M., 1980.
- ⁶⁰R. Kubo and K. J. Tomita, *J. Phys. Soc. Jpn.* **9**, 888 (1954).
- ⁶¹L. D. Landau and E. M. Lifshitz, *Kvantovaya mekhanika*, Nauka, M., 1974 [Engl. Transl., Quantum Mechanics, Pergamon Press, Oxford, 1977].
- ⁶²A. Abragam and B. Bleaney, *Electron Paramagnetic Resonance of Transition Ions*, Clarendon Press, Oxford, 1970 [Russ. Transl., Mir, M., 1972 (v. 1), M., 1973 (v. 2)].
- ⁶³B. Bleaney, *Proc. R. Soc. London A* **370**, 313 (1980).
- ⁶⁴F. L. Aukhadeev, I. I. Valeev, I. S. Konov, V. A. Skrebnev, and M. A. Teplov, *Fiz. Tverd. Tela (Leningrad)* **15**, 253 (1973) [*Sov. Phys. Solid State* **15**, 163 (1973)].
- ⁶⁵R. Yu. Abdulsabirov, I. S. Konov, S. L. Korableva, S. N. Lukin, M. S. Tagirov, and M. A. Teplov, *Zh. Eksp. Teor. Fiz.* **76**, 1023 (1979) [*Sov. Phys. JETP* **49**, 517 (1979)].
- ⁶⁶I. S. Konov and M. A. Teplov, *Fiz. Tverd. Tela (Leningrad)* **18**, 1114 (1976) [*Sov. Phys. Solid State* **18**, 636 (1976)].
- ⁶⁷L. K. Aminov, M. S. Tagirov, and M. A. Teplov, *Zh. Eksp. Teor. Fiz.* **79**, 1322 (1980) [*Sov. Phys. JETP* **52**, 669 (1980)].
- ⁶⁸V. A. Ioffe, S. I. Andronenko, I. A. Bondar', L. P. Mezentseva, A. N. Bazhan, and Ch. Bazhan, *Pis'ma Zh. Eksp. Teor. Fiz.* **34**, 586 (1981) [*JETP Lett.* **34**, 562 (1981)].
- ⁶⁹S. A. Al'tshuler, A. A. Kudryashov, M. A. Teplov, and D. N. Terpilovskii, *Pis'ma Zh. Eksp. Teor. Fiz.* **35**, 239 (1981) [*JETP Lett.* **35**, 299 (1982)].
- ⁷⁰P. L. Scott, H. J. Stapledon, and C. Wainstein, *Phys. Rev. A* **137**, 71 (1965).
- ⁷¹A. V. Egorov, M. V. Eremin, M. S. Tagirov, and M. A. Teplov, *Zh. Eksp. Teor. Fiz.* **77**, 2375 (1979) [*Sov. Phys. JETP* **50**, 1145 (1979)].
- ⁷²A. A. Kudryashov, S. L. Korableva, M. S. Tagirov, and M. A. Teplov, *Fiz. Tverd. Tela (Leningrad)* **25**, 1887 (1983) [*Sov. Phys. Solid State* **25**, 1090 (1983)].
- ⁷³A. V. Egorov, A. A. Kudryashov, M. S. Tagirov, M. A. Teplov, *Fiz. Tverd. Tela (Leningrad)* **26**, 2223 (1984) [*Sov. Phys. Solid State* **26**, 7, 1351 (1984)].
- ⁷⁴M. A. Teplov, *Zh. Eksp. Teor. Fiz.* **55**, 2145 (1968) [*Sov. Phys. JETP* **28**, 1136 (1969)].
- ⁷⁵M. V. Eremin, I. S. Konov, and M. A. Teplov, *Pis'ma Zh. Eksp. Teor. Fiz.* **73**, 569 (1980) [*Sov. Phys. JETP* **46**, 297 (1977)].
- ⁷⁶A. A. Antipin, I. S. Konov, S. L. Korableva, R. M. Rakhmatullin, M. S. Tagirov, M. A. Teplov, and A. A. Fedil', *Fiz. Tverd. Tela (Leningrad)* **21**, 111 (1979) [*Sov. Phys. Solid State* **21**, 65 (1979)].
- ⁷⁷L. K. Aminov, M. S. Tagirov, and M. A. Teplov, *Zh. Eksp. Teor. Fiz.* **82**, 224 (1982) [*Sov. Phys. JETP* **55**, 135 (1982)].
- ⁷⁸L. K. Aminov and M. A. Teplov, *Paramagnitnii rezonans (Paramagnetic Resonance)*, Kazan' (Publ. Univ. Kazan', 1983), no. 19, p. 64.
- ⁷⁹L. K. Aminov, A. A. Kudryashov, M. S. Tagirov, and M. A. Teplov, *Zh. Eksp. Teor. Fiz.* **86**, 1791 (1984) [*Sov. Phys. JETP* **59**, 1042 (1984)].
- ⁸⁰K. Andres, *Cryogenics* **18**, 473 (1978).
- ⁸¹K. Andres, and S. Darack, *Physica, B + C* **86-88**, 1071 (1977).
- ⁸²F. Pobell, *Physica, B* **109-110**, 1485 (1982).
- ⁸³M. Kubota, R. M. Mueller, C. Buchal, H. Chocolacs, J. R. Owers-Bradley, and F. Pobell, *Phys. Rev. Lett.* **51**, 1382 (1983).

- ⁸⁴H. Suzuki, N. Nambudripad, B. Bleaney, A. L. Allsop, G. J. Bowden, I. A. Campbell, and N. J. Stone, *J. Phys. (Paris)* **39**, C6-800 (1978).
- ⁸⁵A. V. Egorov, F. L. Aukhadeev, M. S. Tagirov, and M. A. Teplov, *Pis'ma Zh. Eksp. Teor. Fiz.* **39**, 480 (1984) [*JETP Lett.* **39**, 584 (1984)].
- ⁸⁶R. W. Broach, J. M. Williams, G. P. Felcher, and D. G. Hinks, *Acta Crystallogr. Sect. B* **35**, 2317 (1979).
- ⁸⁷S. A. Al'tshuler and B. M. Kozyrev, *Elektronnii paramagnitnii rezonans soyedinenii elementov promezhutochnykh grupp (Electron Paramagnetic Resonance of Transition-Metal Compounds)*, Nauka, M., 1972.
- ⁸⁸A. I. Burshtein, *Kvantovaya kinetika (Quantum Kinetics)*, Novosibirsk (Publ. Univ. Novosibirsk, 1968), part 1.
- ⁸⁹M. P. Vaisfel'd, *Fiz. Tverd. Tela (Leningrad)* **14**, 737 (1972) [*Sov. Phys. Solid State* **14**, 628 (1972)].
- ⁹⁰R. E. Thoma, G. D. Brunton, R. A. Penneman, and T. A. Keenan, *Inorg. Chem.* **9**, 1096 (1970). I. A. Ivanova, A. M. Morozov, M. A. Petrova, and I. G. Podkolzina, *Izv. Akad. Nauk SSSR Neorg. Mater.* **11**, 2175 (1975).
- ⁹¹L. L. Buishvili, *Zh. Eksp. Teor. Fiz.* **49**, 1868 (1965) [*Sov. Phys. JETP* **22**, 1277 (1966)].
- ⁹²G. R. Khutsishvili, *Usp. Fiz. Nauk* **96**, 441 (1968) [*Sov. Phys. Usp.* **11**, 802 (1969)].
- ⁹³A. Abragam and M. Goldman, *Rep. Prog. Phys.* **41**, 395 (1978).
- ⁹⁴M. Borghini, *Phys. Rev. Lett.* **16**, 318 (1966).
- ⁹⁵L. A. Bumagina, V. I. Krotov, B. Z. Malkin, and A. Kh. Khasanov, *Zh. Eksp. Teor. Fiz.* **80**, 1543 (1981) [*Sov. Phys. JETP* **53**, 792 (1981)].
- ⁹⁶L. K. Aminov, *Spektroskopiya kristallov (Spectroscopy of Crystals)*, Nauka, L., 1978, p. 116.
- ⁹⁷B. Bleaney, G. A. D. Briggs, J. F. Gregg, G. H. Swallow, and J. M. R. Weaver, *Proc. R. Soc. London A* **388**, 479 (1983).
- ⁹⁸L. K. Aminov, *Fiz. Tverd. Tela (Leningrad)* **23**, 2167 (1981) [*Sov. Phys. Solid State* **23**, 1266 (1981)].
- ⁹⁹M. T. Huiku and M. T. Lopenen, *Phys. Rev. Lett.* **49**, 1288 (1982).
- ¹⁰⁰J. Roinel, V. Bouffard, G. L. Bachella, M. Pinot, P. Meriel, P. Roubeau, O. Avenel, M. Goldman, and A. Abragam, *Phys. Rev. Lett.* **41**, 1572 (1978).
- ¹⁰¹P. C. Hammel, M. L. Rourke, Y. Hu, T. J. Gramila, T. Mamiya, and R. C. Richardson, *Phys. Rev. Lett.* **51**, 21 (1983).

Translated by F. J. Crowne